Effects of High-Fat Feeding on Skeletal Muscle Insulin Signalling in Sarcolipin Knockout Mice

by

Ryan Sayer

A thesis
presented to the University of Waterloo
in fulfillment of the
thesis requirement for the degree of
Master of Science
in
Kinesiology

Waterloo, Ontario, Canada, 2010

AUTHOR'S DECLARATION

I hereby declare that I am the sole author of this thesis. This is a true copy of the thesis, including any required final reversions, as accepted by my examiners.

I understand that my thesis may be made electronically available to the public.

Ryan Sayer

ABSTRACT

Type II diabetes mellitus (T2DM) has been associated with the onset of diet-induced obesity, which is currently on the rise worldwide. T2DM is typically characterized by insulin resistance in peripheral tissues such as adipose tissue, liver, and skeletal muscle. In skeletal muscle it is widely accepted that the defective insulin action is due to the inability of the cell to sufficiently activate the insulin signalling pathway and promote systemic glucose uptake. The sarcolipin-null (KO) mouse is a potential novel model for diet-induced obesity and diabetes. KO mice become significantly more obese and display a greater glucose intolerance than wildtype (WT) mice following an 8-week high-fat diet (HFD; 42% calories from fat) but the underlying mechanisms are still unknown.

In this study the role of defective skeletal muscle insulin signalling in the development of the impaired glucose tolerance in KO mice was investigated. It was hypothesized that the HFD fed KO mice would exhibit greater reductions in IRS1 tyr^{628} and Akt ser^{473} phosphorylation (i.e. decreased activation of the insulin signalling pathway) than controls. Furthermore, it was believed that KO mice would display increased phosphorylation of IRS1 ser^{307}, which is commonly associated with insulin resistance. At 16-weeks of age KO mice and littermates were subdivided into two groups and placed on either a HFD (n=30) or chow diet (n=24) for an 8-week period. Changes in body weight, glucose tolerance, and insulin tolerance were assessed pre- and post-diet period. Following the completion of the diet intervention mice were treated with an intraperitoneal injection of insulin (0.75U/kg) or vehicle solution and sacrificed for tissue collection. Epididymal/inguinal and retroperitoneal fat pads were removed for assessment of whole body adiposity. Whole gastrocnemius muscle was excised and homogenized for Western blot analysis of several key proteins of the insulin signalling cascade.

Following completion of the HFD KO mice (48.6 ± 1.6 g) weighed significantly more than HFD fed wildtype (WT) mice (41.5 ± 1.6 g), and all chow fed mice (KO: 36.8 ± 1.5 g; WT: 35.2 ± 1.2 g; $p<0.001$). Glucose tolerance testing showed that KO mice exhibited significantly greater glucose intolerance compared to control mice post-HFD ($p<0.001$). Insulin tolerance testing, however, revealed no change in insulin sensitivity in KO or WT mice post-HFD ($p>0.05$). The HFD fed KO mice (0.73 ± 0.06 g) had an elevated retroperitoneal fat pad weight than HFD fed WT (0.49 ± 0.05 g) and all chow fed mice (KO: 0.28 ± 0.04 g; WT:

0.24 ± 0.04 g; $p<0.01$). Western blot analysis revealed a similar reduction in insulin receptor substrate-1 (IRS1) tyr^{628} phosphorylation in both KO and WT mice following the HFD (Con WT: 2.82 ± 0.69; Con KO: 3.06 ± 0.73; HFD WT: 1.71 ± 0.28; HFD KO: 1.28 ± 0.11 fold increase over non-insulin stimulated mice; $p<0.02$). IRS1 ser^{307} phosphorylation was elevated in both genotypes post-HFD (HFD WT: 2.97 ± 1.19; HFD KO: 2.17 ± 0.59 fold increase over standard chow fed control mice; $p<0.03$). Insulin treatment did not stimulate phosphorylation of Akt ser^{473} in KO or WT mice regardless of diet ($p>0.05$). In summary there was no difference between KO and WT mice in skeletal muscle insulin sensitivity as assessed by the phosphorylation of insulin signalling intermediates. An increase in IRS1 ser^{307} phosphorylation appears to be the primary mechanism for the reduced activation of IRS1 following the HFD in both KO and WT mice. However, the results from the current investigation did not support the notion that impaired skeletal muscle insulin signalling is responsible for the more pronounced diet-induced glucose intolerance observed in KO mice. Future studies investigating the viability of skeletal muscle GLUT4 translocation and glucose uptake as well as the glucose-induced insulin secretion of pancreatic β-cells following consumption of a HFD would help elucidate the mechanism of glucose intolerance in KO mice.

ACKNOWLEDGEMENTS

Over the years my journey through the Kinesiology undergraduate and graduate programs at the University of Waterloo has been an extraordinary experience. However, I would not have endured this endeavor without the support of my family – Patricia, Ronald, Graehem, and Amber. They provided the strength needed to complete this undertaking.

I would also like to acknowledge my supervisor, Dr. Russell Tupling, for granting me the privilege to join his laboratory nearly 4 years ago. I cannot sufficiently express the sheer gratitude that I owe Dr. Tupling for the countless opportunities, the insights and guidance, and the support that he has provided; all of which have undoubtedly contributed to my recent admission to the Faculty of Medicine at the University of Toronto.

I was very fortunate to have had the opportunity to benefit from the tutelage from my fellow lab mates Dr. Eric Bombardier and Chris Vigna. I also cannot forget to mention the significant contribution that Daniel Gamu and Anton Trihn have made to this thesis project. I am truly thankful for all of their expertise and assistance.

The donation of *Sln-null* mice by Dr. Muthu Periasamy at Ohio State University was also greatly appreciated as it allowed for the creation of a breeding colony at the University of Waterloo.

The successful completion of this thesis document reflects the culmination of years of guidance, encouragement, and support from countless friends and family. I would not be in the position I am today without them.

DEDICATION

This thesis is dedicated to my family – my parents, Ronald and Patricia; my brother, Graehem; and my dearest, Amber. The love and encouragement that they have provided throughout the years has undoubtedly contributed to my success.

To my beloved friend, Annie – your resolve was an inspiration to us all. You are dearly missed, but never forgotten.

TABLE OF CONTENTS

CONCLUSIONS

LIST OF FIGURES

LIST OF ABBREVIATIONS

AS160 - Akt substrate of 160 kDa

ATP – adenosine triphosphate

BMI – body mass index

Ca^{2+} –calcium ion

CPA – cyclopiazonic acid

DAG - diacylglyceride

DGAT1 - diacylglyceride transferase-1

HFD – high fat diet

GAP - GTPase activating protein

GLUT4 – glucose transporter type 4

GSV - GLUT4 storage vesicles

GTP - guanosine triphosphate

GTT – glucose tolerance test

IMTG - intramuscular triglyceride

IR – insulin receptor

IRS1 – insulin receptor substrate 1

ITT – insulin tolerance test

KO – knockout/ homozygous-null mouse

LCACoA - long chain acyl-CoA fatty acid

NEFA – non-esterified fatty acid

OLETF - Otsuka Long-Evans Tokushima fatty rat

PI2P - phosphatidylinositol-3,4-bisphosphate

PI3P – phosphatidylinositol-3,4,5-triphosphate

PI3K - phosphatidylinositol 3-kinase

PDK1 - phosphoinositide-dependent kinase-1

PKC – protein kinase C

PVDF – polyvinylidene difluoride

SDS - Sodium dodecyl sulphate

SER - serine

SERCA – sarco(endo)plasmic reticulum Ca^{2+} ATPase

SLN – sarcolipin

SR – sarcoplasmic reticulum

T2DM – Type II diabetes mellitus

TAG – triacylglycerol

TYR- tyrosine

UCP-3 – uncoupling protein 3

WT– wild type

ZDF - Zucker Diabetic fatty rat

1.0 OBESITY & DIABETES

1.1 Introduction to Obesity

Over the past 20 years the incidence of obesity has progressively increased and current evidence suggests that this epidemic will continue to escalate (Katzmarzyk & Mason, 2006). In Canada, recent estimates indicate that 35% of the nation's population is classified as overweight while 15% is considered obese (Katzmarzyk & Mason, 2006), which is most likely a conservative estimate as self-reported measures typically underestimate the actual incidence of obesity (Rowland, 1990; Tjepkema, 2006; Merrill & Richardson, 2009). The high prevalence of obesity has translated into an annual estimated cost of $4.3 billion on the Canadian health care system (Katzmarzyk & Janssen, 2004).

The hallmark characteristic associated with obesity is an inappropriate fat accumulation primarily as a result of a chronic positive energy imbalance (Schrauwen, 2007) and typically diagnosed by an individual's body mass index (BMI). BMI (body weight (kg) / height (m^2)) is a common surrogate measure for percent body fat (Deurenberg et al., 2001) that is used to assess potential abnormalities in body composition as determined by the World Health Organization guidelines. One of the most accurate methods for determining differences in body composition, particularly in humans, is the use of the dual-energy x-ray absorptiometry technique (Mattsson & Thomas, 2006).

The development of coronary heart disease and stroke, hypertension, gall bladder disease, some types of cancer (breast, colon, and prostate), and respiratory dysfunction have all been strongly associated with increased adipose tissue mass and obesity (Flegal et al., 2007; Kopelman, 2007; Blakemore & Froguel, 2008). Obesity has also been found to be an independent risk factor for the development of type II diabetes (Must et al., 1999) as 80% of type II diabetics are obese (Bloomgarden, 2000). The presence of obesity appears to predispose individuals to an accumulation of lipid metabolites in insulin sensitive tissues and subsequent insulin resistance, which will be discussed in further detail in Section 3.0 Insulin Resistance (Morino, Petersen, & Shulman, 2006).

1.2 Introduction to Diabetes

Diabetes is a metabolic disorder characterized by the presence of hyperglycemia due to insufficient insulin release, defective insulin action, or both (Alberti & Zimmet, 1998). The most common form of diabetes is non-insulin dependent diabetes mellitus, otherwise referred to as type II diabetes mellitus (T2DM) or adult-onset diabetes (Alberti & Zimmet, 1998). The primary characteristic of T2DM is an inadequate response to insulin by the peripheral tissues such as skeletal muscle, adipose tissue, and the liver despite near normal levels of pancreatic insulin release (Alberti & Zimmet, 1998). Over time, insulin resistance can lead to a chronic elevation of the plasma glucose level, otherwise known as hyperglycemia (Alberti & Zimmet, 1998; Karlsson & Zierath, 2007).

The International Diabetes Federation states that someone is diagnosed with diabetes every five seconds somewhere in the world (IDF, 2007). In 2000, the global prevalence of diabetes was estimated to be at 2.8% of the population, or 171 million people (Wild, Roglic, Green, Sicree, & King, 2004) which is significantly lower than the estimated incidence of T2DM in Canada (Lipscombe & Hux, 2007). It is projected that the worldwide prevalence will more than double to 366 million people by the year 2030 (Wild, Roglic, Green, Sicree, & King, 2004). Diabetes is the fifth leading cause of death in developing countries worldwide (CDA, 2008); diabetics experience a life expectancy that is 5-15 years less than healthy individuals (CDA, 2008).

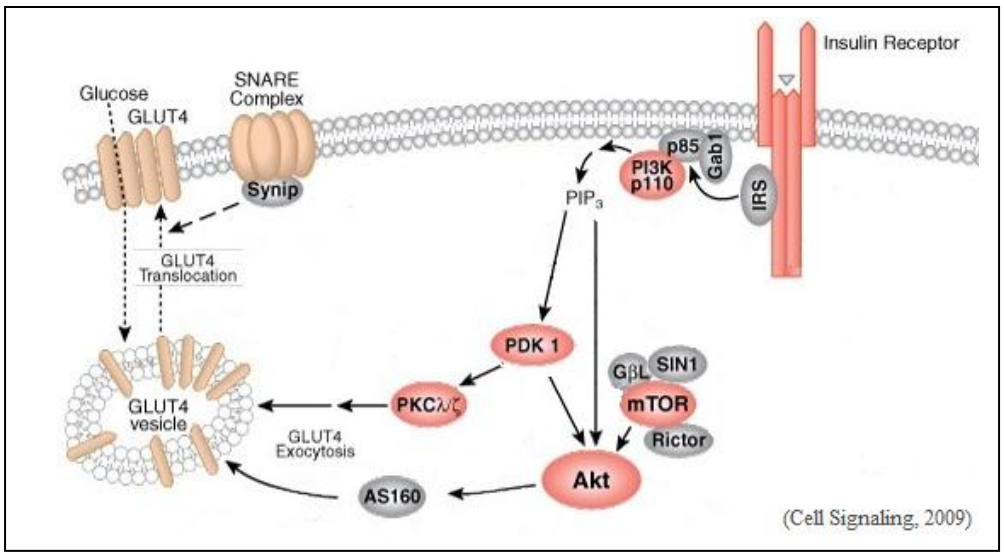

Figure 2.1: Insulin Signaling Pathway in Skeletal Muscle (Cell Signaling, 2009)

2.0 Insulin Signalling in Skeletal Muscle

Skeletal muscle is the primary target of insulin-stimulated glucose uptake in diabetic and non-diabetic individuals (Shulman et al., 1990). In the classic study by DeFronzo et al. (1981), skeletal muscle accounted for 75% of exogenous glucose uptake during insulin infusion. The process by which insulin stimulates glucose uptake is a complex, multi-stepped process which ensures the tight regulation of plasma glucose levels. As seen in Figure 2.1, insulin elicits its effect on skeletal muscle through a series of phosphorylation processes that link the initial binding of insulin to the insulin receptor on the sarcolemma through the translocation of glucose transporters (GLUT) to the cell membrane surface and increase in glucose uptake into the cell (Krook, Wallberg-Henriksson, & Zierath, 2004).

2.1 Insulin Receptor

Insulin receptors (IR) are found embedded in the cell membrane of all insulin responsive tissues such as adipose tissue, the liver, and skeletal muscle. The IR is composed of 4 major peptide-subunits: 2 extracellular alpha-subunits of 135-kDa to which insulin can bind, and 2 intracellular 95-kDa beta-subunits (Borge et al., 2002). Upon insulin binding to the alpha-subunits, the tyrosine kinase domain on the beta-subunits of the IR exhibits autophosphorylation capabilities and rapidly phosphorylates several key tyrosine residues located along the beta-subunit. This activated form of the IR provides docking sites for the

binding of several downstream signalling molecules including the insulin receptor substrates (Karlsson & Zierath, 2007).

2.2 Insulin Receptor Substrate

Insulin receptor substrates (IRS-1 to 4) act as docking proteins for a variety of insulin responsive molecules and function as key mediators of the insulin signal. The tissue distribution and functional role of each IRS isoform varies throughout the body, however IRS recruitment occurs in a similar fashion. Each IRS protein contains a phosphotyrosine binding (PTB) domain that will bind to the phosphorylated tyrosine residues on the IR (Karlsson & Zierath, 2007). Upon IRS binding the kinase activity of the activated IR will phosphorylate several tyrosine residues within a tyrosine-methionine-X-methionine (YMXM) motif on IRS which activates the protein (Shoelson et al., 1992, Karlsson & Zierath, 2007). The phosphorylated YMXM motif provides a suitable docking site for downstream intermediates of the insulin signalling cascade containing src-homology 2 (SH2) domains, such as phosphatidylinositol 3-kinase (Sun et al., 1991; Shoelson et al., 1992; Karlsson & Zierath, 2007).

In skeletal muscle IRS-1 and IRS-2 are the predominantly expressed isoforms of the protein involved in the regulation of glucose homeostasis. Determining the specific function of each IRS protein has proven difficult since the high sequence similarity and partial functional redundancy between the isoforms allow for potential compensations to occur. For instance, IRS-1 transgenic knockout mice exhibit only mild peripheral insulin resistance due to a compensatory up-regulation of IRS-3 (Kaburagi et al., 1997). Nonetheless, recent findings indicate that each protein has exclusive signalling roles.

In L6 myotubes, a reduction of either IRS-1 or IRS-2 by small interfereing RNA gene silencing revealed that IRS-1 mediates GLUT4 translocation and glucose uptake while IRS-2 has no effect on these parameters (Huang et al., 2005). Furthermore, in heterozygous null rodents for the gene coding for either IR/IRS-1 or IR/IRS-2, the former develop severe insulin resistance in skeletal muscle while the latter show severe insulin resistance of the liver (Kido et al., 2000). Complete knockout of the IRS-2 gene in mice leads to the development of T2D primarily from a reduced pancreatic β-cell mass and insufficient insulin release even though moderate whole body insulin resistance is reported in the liver and skeletal muscle (Withers et

al., 1998). These results suggest that IRS-1 is the predominant isoform mediating signal transduction in skeletal muscle while IRS-2 is thought to be important in pancreatic β-cell development and hepatic signalling processes. In humans IRS-2 may have a slightly larger role in skeletal muscle insulin signalling than in rodent models since the human IRS-3 gene is non-functional (Krook, Wallberg-Henriksson, & Zierath, 2004).

2.3 Phosphatidylinositol 3-Kinase

Phosphatidylinositol 3-kinase (PI3K) is an essential intermediary protein in the insulin signalling pathway of glucose uptake (Krook, Wallberg-Henriksson, & Zierath, 2004). PI3K is composed of a 110-kDa catalytic subunit (p110) and one of several regulatory subunits (p85α, p85β, p55α, p50α, or p55γ). The most predominant regulatory subunit in insulin sensitive tissue is the p85α subunit which comprises 70-80% of the total regulatory subunits in these tissues (Ueki et al., 2002; Ueki et al., 2003).

The regulatory subunit contains a SH2 domain that binds phosphorylated tyrosine residues with a high affinity (Karlsson & Zierath, 2007). Upon tyrosine phosphorylation of IRS, the regulatory subunit of PI3K binds to the activated IRS and the newly formed protein complex migrates towards the plasma membrane. Following migration, the p110 subunit phosphorylates the 3'-OH position of the inositol ring of plasma membrane inositol phospholipids converting phosphatidylinositol-3,4-bisphosphate (PI2P) to PI-3,4,5-triphosphate (PI3P) (Karlsson & Zierath, 2007). The increase of plasma membrane PI3P initiates the recruitment of proteins containing pleckstrin homology domains to the cell surface such as protein kinase B/Akt and phosphoinositide-dependent kinase-1 (PDK1) (Leney & Tavare, 2009).

2.4 Protein Kinase B/Akt

Protein kinase B, also known as Akt, is a serine/threonine kinase that has been found to be a central intermediate for several metabolic pathways downstream of PI3K such as in the activation of glycogen synthase kinase-3 (Karlsson & Zierath, 2007). Akt has also been shown to have a critical role in GLUT4 translocation and glucose transport in adipocytes and L6 myotubes (Tanti et al., 1997).

There are three isoforms of Akt found in skeletal muscle (Akt1, Akt2, and Akt3). Investigations utilizing isoform specific knockout models have revealed specialized functional roles for each isoform. From these studies, Akt2 deficiency leads to the development of insulin resistance and diabetes-like symptoms, and therefore appears to play an essential role in insulin signalling and glucose uptake (Cho et al., 2001a). On the other hand, Akt1 was required for normal growth but did not have a significant influence on glucose homeostasis in mice (Cho et al., 2001b).

One of the key features of Akt is that its N-terminus contains a pleckstrin homology domain that favours the binding of phosphatidylinositol lipids, such as PI3P. Thus, Akt will re-localize to the cell membrane upon the production of PI3P by PI3K, which compartmentalizes the serine/threonine kinase to the area of insulin signalling. (Karlsson & Zierath, 2007)

Once anchored to the cell membrane through its interaction with PI3P, Akt undergoes two phosphorylation steps to reach complete activation (Alessi et al., 1996). First, Akt is phosphorylated on its C-terminus at Ser^{473} by mTOR:Rictor:GbL complex (Sarbassov et al., 2005). Additionally, PDK1, which is allosterically activated by PI3P, phosphorylates the catalytic domain of Akt at Thr308 (Alessi et al., 1997; Krook, Wallberg-Henriksson, & Zierath, 2004).

2.5 Akt Substrate of 160 kDa

It has been well established that insulin mediates the translocation of GLUT4 to the cell membrane and increases glucose uptake (Leney & Tavare, 2009); however, the exact mechanistic steps that link the activation of Akt to the recruitment of GLUT4 has remained elusive. Recently, Sano et al. (2003) reported the discovery of a novel insulin-activated Akt substrate of 160 kDa, subsequently named AS160.

AS160 was first implicated as a mediator of glucose uptake upon observations that point mutations at two or more of the phosphorylation sites on AS160 significantly reduced insulin-stimulated GLUT4 translocation (Sano et al., 2003). Additionally, reducing the content of AS160 in 3T3-L1 adipocytes causes a 2-fold increase in cell surface GLUT4 and glucose uptake without insulin stimulation (Gonzalez & McGraw, 2006). Karlsson et al. (2005) have also shown that insulin-stimulated AS160 phosphorylation is significantly reduced in skeletal muscle from T2D patients.

There are five potential sites of phosphorylation (3 serine and 2 threonine residues) on AS160 in response to insulin (Sano et al., 2003). AS160 also contains a GTPase activating protein (GAP) domain for a Rab (Sano et al., 2003). Rabs are small G proteins that are commonly cited to regulate many cellular processes involving vesicle formation, movement, and fusion (Zerial & McBride, 2001). More recently, Rabs 8A and 14 have been implicated in GLUT4 translocation in muscle and are regulated by the GAP domain of AS160 (Miinea et al., 2005; Ishikura et al., 2007).

Interestingly, Sano et al. (2003) also reported that insulin-stimulated GLUT4 translocation was preserved following the point mutations of the phosphorylation sites of AS160 when an additional mutation within the GAP domain was present. This provides a strong indication that AS160 requires a functional GAP domain to inhibit glucose uptake.

The proposed mechanism by which AS160 regulates GLUT translocation is quite interesting as the recruitment of AS160 differs from the other insulin signalling intermediates. Presumably the non-phosphorylated form of AS160 is considered to be the active structure and restricts GLUT translocation to the cell surface. It is proposed that a guanosine triphosphate (GTP)-bound Rab molecule is necessary for GLUT translocation. The activated GAP domain of the non-phosphorylated AS160 hydrolyses the Rab-GTP to GDP and prevents GLUT translocation (Cartee & Wojtaszewski, 2007). Insulin stimulation, and subsequent PI3K and Akt activation, inhibits the activity of the GAP domain through the phosphorylation of several serine/threonine residues on AS160 (Bruss et al., 2005; Cartee & Wojtaszewski, 2007). Inactivation of the AS160 GAP domain prevents the hydrolysis of the nearby GTP-bound Rab and GLUT translocation will occur.

2.6 Glucose Transport

Insulin has been established to stimulate an increase of glucose uptake in skeletal muscle and adipose tissue for over 50 years (Park & Johnson, 1955). However, it was not until decades later that insulin was observed to promote the movement of a glucose transport system from intracellular stores to the plasma membrane (Cushman & Wardzala, 1980; Suzuki & Kono, 1980).

Glucose transporters (GLUT) are members of the facilitated diffusion carrier family, and assist glucose and other hexose sugars to cross a cellular membrane barrier along a

concentration gradient (Mueckler, 1994; Augustin, 2010). There are fourteen members of the GLUT family (1-14) which have a wide distribution of expression throughout the body (Mueckler, 1994; Augustin, 2010).

In skeletal muscle two GLUT transporters, namely GLUT1 and GLUT4, are the primary transporters responsible for glucose uptake (Mueckler, 1994; Augustin, 2010). GLUT1 is permanently expressed at low levels within the plasma membrane of skeletal muscle, where it supplies the cell with sufficient levels of glucose for basal cellular processes (Mueckler, 1994; Augustin, 2010). GLUT4 is recognized as the primary glucose transporter isoform responsible for the enhanced glucose uptake following insulin stimulation (Charron et al., 1989; Fukomoto et al., 1989; James et al., 1989). During the basal cellular state less than 5% of the total GLUT4 pool is found on the plasma membrane whereas up to 50% of the total GLUT4 pool can be found embedded in the cell surface following insulin stimulation (Leney & Tavare, 2009).

The majority of the work characterizing the location of the intracellular GLUT4 stores has been performed on 3T3-L1 adipocytes thereby questioning the applicability of the findings *in vivo*. Nonetheless, GLUT4 vesicles have been observed to be situated throughout subcellular portions of the cytoplasm and the perinuclear region of the cell, as well as in sections near the plasma membrane indicating that GLUT4 vesicles are localized to several distinct intracellular pools within the cell (Bornemann et al., 1992; Leney & Tavare, 2009).

The insulin-stimulated increase of GLUT4 vesicles from intracellular pools to the plasma membrane can be explained by two plausible models: the dynamic and the static model of GLUT translocation (Fig. 2.2). In the dynamic model of GLUT4 translocation, the total pool of GLUT4 vesicles are thought to be continuously cycling between the intracellular compartments and the plasma membrane. During basal cellular conditions a slow, steady state of GLUT4 exocytosis and endocytosis is achieved which ensures a constant rate of glucose uptake and maintenance of plasma glucose homeostasis (Leney & Tavare, 2009). Insulin stimulation increases the rate of GLUT4 exocytosis in order to increase the number of GLUT4 molecules on the plasma membrane (Leney & Tavare, 2009).

The static model of GLUT4 translocation proposes that under basal conditions there are a limited number of GLUT4 vesicles available to cycle between the cell surface and intracellular stores. Thus, glucose uptake remains low. Insulin action on skeletal muscle

recruits additional GLUT4 vesicles into the cycling pool from the intracellular stores thereby increasing the total number of GLUT4 vesicles available to fuse with the plasma membrane and increase the rate of glucose uptake (Leney & Tavare, 2009).

In either case it is believed that insulin elicits its action through the insulin signalling cascade and subsequent inactivation of AS160 (Larance et al., 2005). The active form of AS160 is thought to be bound to the GLUT4 storage vesicles (GSV) under basal conditions. Deactivation of the Rab GAP domain upon insulin stimulation leads to the dissociation of AS160 from the GSV which allows the translocation of GLUT4 to the cell surface.

In the absence of insulin, GLUT4 vesicles located near the cell surface unsuccessfully attempt to bind to the plasma membrane (Bai et al., 2007). The dissociation of AS160 from the GLUT4 vesicle enables the GTP form of Rab to bind to the vesicle. The Rab-GTP complex will bind to Rip11 and provide a docking site on the GSV that will interact with acidic phospholipids in the plasma membrane (Bai et al., 2007; Leney & Tavare, 2009). GLUT4 is incorporated into the plasma membrane following the docking of the GSV which increases glucose uptake into the cell.

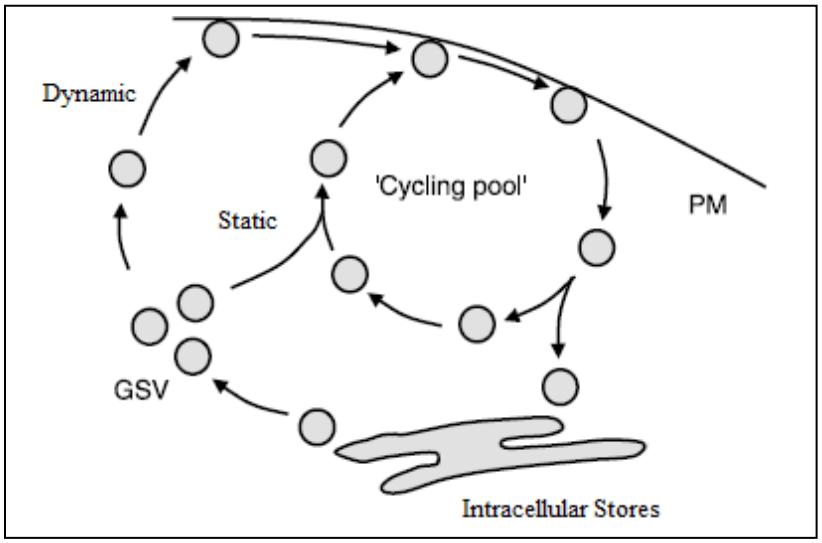

Figure 2.2: Proposed Models of GLUT translocation (Leney & Tavare, 2009)

3.0 Introduction to Insulin Resistance in Skeletal Muscle

One of the early events in the development of T2DM is the inability of insulin to promote peripheral glucose disposal into skeletal muscle and suppress hepatic production (Warram et al., 1990; Lillioja et al., 1993; Boden, 2001; DPPRG, 2005; Timmers, Schrauwen, & de Vogel, 2007). Insulin resistance has been well established to be associated with obesity as lean non-diabetic individuals are approximately two times more insulin sensitive than obese non-diabetics (Damsbo et al., 1991; Ferrannini et al., 1997; Boden, 2001).

Originally it was believed that the impairment within skeletal muscle was due to a reduced capacity of hexokinase or glycogen synthase activity since an approximate 50% decrease in insulin-stimulated muscle glycogen synthesis is observed for T2DM (Shulman et al., 1990). However, it has since been reported that a reduction in the insulin-stimulated glucose transport appears to be the primary malfunction in the insulin signalling system and the cause for the onset of hyperglycemia (Cline et al., 1999; Cline et al., 2002; Fueger et al., 2004).

There is a strong inverse correlation between insulin sensitivity and body fat mass as sensitivity decreases with weight gain and normalizes with reductions in fat mass (Sims et al., 1973; Boden et al., 1993; Boden, 2001). Lipid infusion studies have revealed a close association between elevated plasma non-esterfied fatty acids (NEFAs) and impaired insulin sensitivity (Boden et al., 1991; Perseghin et al., 1997; Itani et al. 2002), and can produce defects in insulin-stimulated glucose transport due to the reduced tyrosine phosphorylation of IRS-1 (Boden & Chen, 1995; Dresner et al., 1999; Yu et al., 2002). Additionally, lowering chronically elevated plasma NEFAs with the anti-lipolytic drug Acipimox in obese non-diabetic and obese diabetic individuals (both with impaired insulin sensitivity compared to lean controls) doubled insulin sensitivity in both groups (Santomauro et al., 1999). Taken together these results suggest a possible role of excess NEFAs in the onset of insulin resistance.

The plasma NEFA hypothesis does fit the obesity-induced diabetes model as elevated plasma NEFA levels are common characteristics of obesity and insulin resistance (Gorden, 1960; Reaven et al., 1988; Boden, 1997). However, in the lipid infusion studies there is a 3-4 hour delay between the acute elevation of plasma NEFAs and the onset of insulin resistance; the insulin resistance also persists hours after the lipid infusion has stopped (Boden et al., 1991; Boden, 2001; Itani et al. 2002). Interestingly, changes in plasma NEFAs are linearly correlated

to intramuscular triglyceride (IMTG) levels and insulin resistance (Boden, 2001). Boden et al. (2001) have demonstrated that there is a dose-dependent increase in IMTG content following an acute elevation of plasma NEFA. The elevated IMTG was measured 4-hours after lipid infusion suggesting that plasma NEFA may need to be transported into skeletal muscle and re-esterified before insulin sensitivity is affected (Boden et al., 2001).

3.1 Intramuscular Lipid Accumulation

There has been a growing body of evidence for the role of aberrant lipid accumulation, particularly IMTG, in the onset of skeletal muscle insulin resistance (Shulman, 2000; Schmitz-Peiffer, 2000). High-fat diet (HFD) fed mice exhibit symptoms of insulin resistance with an associated increase of IMTG content (Kraegen et al., 1991; Oakes et al., 1997; Dobbins et al., 2001) whereas reducing IMTG content through caloric restriction improved insulin sensitivity in T2DM patients (Lara-Castro et al., 2008).

However, not all insulin resistance is associated with elevated IMTG indicating that IMTG content cannot be the sole culprit in the onset of insulin resistance (Befroy et al., 2007). For example, the upregulation of the triglyceride synthesis enzyme diacylglyceride transferase-1 (DGAT1) in mice increases IMTG content but improves muscle insulin sensitivity (Liu et al., 2007). Moreover, moderate intensity endurance exercise in humans increases DGAT1 expression and IMTG content while improving insulin sensitivity (Phillips et al., 1996; Schenk & Horowitz, 2007). Interestingly, highly-trained elite endurance athletes have been found to exhibit severely elevated IMTG measures while exhibiting increased insulin sensitivity (Goodpaster et al., 2001; Kiens, 2006). Thus, it appears that IMTG content is merely associated with the degree of insulin resistance rather than directly causing insulin resistance. More likely, specific IMTG lipid intermediates such as long chain acyl-CoA fatty acids (LCACoAs), ceramides, & diacylglycerides (DAGs) elicit a direct, negative impact on the insulin signalling cascade and impair glucose uptake as depicted in Figure 3.1 (Shulman, 2000; Kraegen & Cooney, 2008).

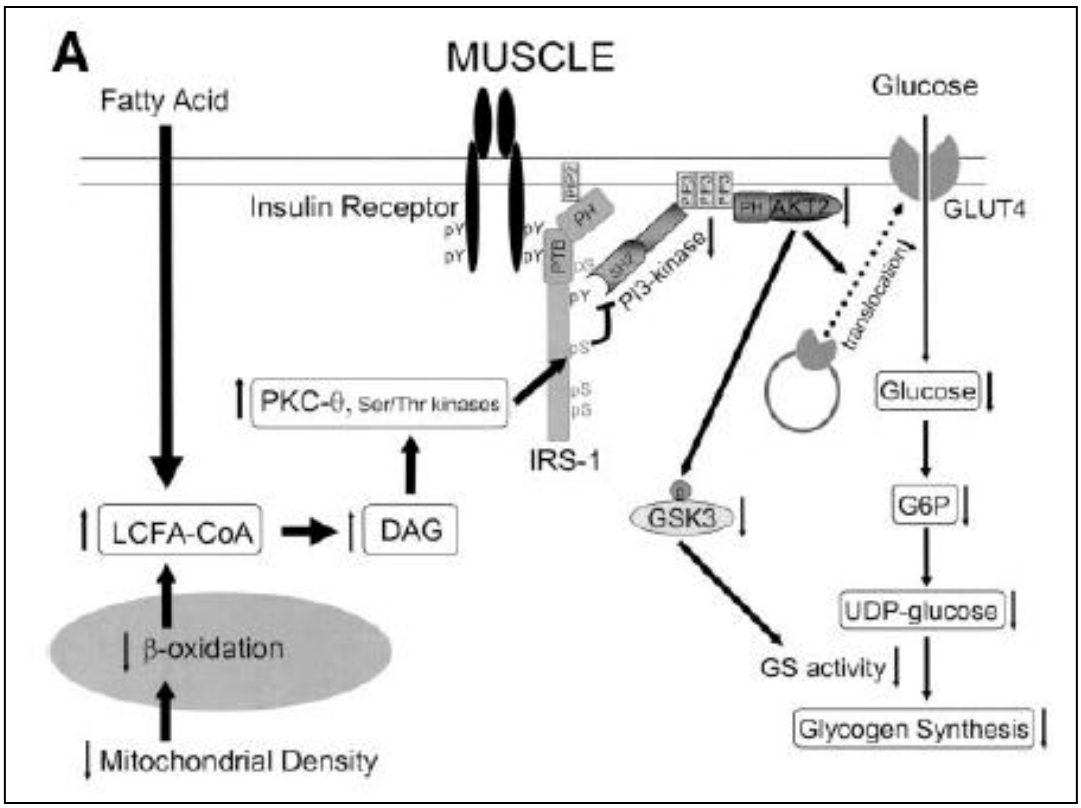

Figure 3.1: Proposed Mechanism of Insulin Resistance in Skeletal Muscle (Morino, Petersen, & Shulman, 2006)

3.1.1 Long chain acyl-CoA

Typically, LCACoAs are transported into the mitochondria for energy production (Timmers, Schrauwen, & de Vogel, 2007). LCACoAs have also been shown to modify hexokinase activity (Timmers, Schrauwen, & de Vogel, 2007), and allosterically activate several protein kinase-C (PKC) isozymes (Orellana et al., 1990; Nesher & Boneh, 1994). The activation of PKC suggests a plausible mechanism linking the elevation of LCACoA to the onset of insulin resistance as PKC has been shown to interfere with the insulin signalling pathway (Ellis et al., 2000; Thompson et al., 2000; Morino, Petersen, & Shulman, 2006). Similarly, decreasing the LCACoAs concentration in skeletal muscle through dietary restrictions improves insulin sensitivity (Oakes et al., 1997). However, LCACoAs may solely be a marker of insulin resistance (as suggested with IMTG content) as LCACoA content is closely associated with increased intramuscular ceramide & DAG content (Timmers, Schrauwen, & de Vogel, 2007).

3.1.2 Ceramides

The de novo synthesis of ceramides is dependent upon 4 regulated enzymatic steps commencing with the rate-limiting condensation reaction of serine and palmitoyl-CoA by serine palmitolytransferase (Merrill, 2002; Timmers, Schrauwen, & de Vogel, 2007). Ceramides are common signalling molecules within a cell which mediate various processes such as inhibition of cell division and stimulation of apoptosis (Timmers, Schrauwen, & de Vogel, 2007). Elevated ceramide concentrations have been associated with skeletal muscle insulin resistance in animal models and men at high risk for developing T2DM (Turinsky, O'Sullican, & Bayly, 1990; Adams et al., 2004; Straczkowski et al., 2007), and with fatty acid induced insulin resistance in vitro in cell culture studies (Pickersgill et al., 2007; Sabin et al., 2007). In contrast, inhibtion of de novo ceramide synthesis in Zucker diabetic fatty rats improved insulin sensitivity and lowered the associated ceramide concentration in skeletal muscle (Holland et al., 2007b). Ceramides elicit their effects downstream of IRS1 by promoting the dephosphorylation of Akt by protein phosphatase 2A (Dobrowsky et al., 1993; Schmitz-Peiffer, Craig, & Biden, 1999; Stratford et al., 2004; Holland et al., 2007a) which prevents the translocation of Akt from the cytoplasm to the plasma membrane (Stratford et al., 2004). Thus, insulin-stimulated glucose transport is reduced. Inhibition of de novo ceramide synthesis restores Akt activation and subsequent glucose uptake following insulin stimulation (Chavez et al., 2003; Holland et al., 2007a).

3.1.3 Diacylglycerides

As previously discussed with ceramides, DAGs are a common secondary messenger molecule within cells (Timmers, Schrauwen, & de Vogel, 2007). However, elevated levels of DAGs within muscle from acute lipid infusion or high-fat diets are associated with insulin resistance (Morino, Petersen, & Shulman, 2006; Timmers, Schrauwen, & de Vogel, 2007). Increasing intramuscular DAG content by inhibiting its primary catabolic enzyme (i.e. DAG kinase) results in impaired insulin signalling and glucose uptake, and mild obesity (Chibalin et al., 2008). There are several different reactions that produce DAGs; however, in models of lipid-induced insulin resistance the primary source of the elevated intramuscular DAG concentration is proposed to originate from the esterification of two LCACoAs with glycerol-3-phosphate, and from the hydrolysis of triacylcerides (TAGs) (Timmers, Schrauwen, & de

Vogel, 2007). It is believed that DAGs transmit their effects on the insulin signalling cascade by activating the serine/threonine kinase, protein kinase C-θ (PKCθ) (Chalkey et al., 1998; Schmitz-Peiffer, 2000; Morino, Petersen, & Shulman, 2006).

3.1.4 Protein Kinase-Cθ

Protein kinase-C (PKC) is a common component of cell functions such as cell proliferation, transmembrane ion transport, smooth muscle contraction, and glucose and lipid metabolism (Schmitz-Peiffer, 2000). However, PKCθ is regarded as the primary isozyme in skeletal muscle insulin resistance (Donnelly et al., 1994; Griffin et al., 1999) as aberrant PKCθ activation has been consistently shown to occur in conjunction with an accumulation of intramuscular lipids and insulin resistance (Morino, Petersen, & Shulman, 2006). PKCθ has also been shown to be associated with T2DM (Itani et al., 2001). Furthermore, PKCθ-null mice have been shown to be resistant to diet-induced insulin resistance (Kim et al., 2004). Nevertheless, other PKC isoforms may have a role in insulin resistance, particularly in humans, as PKCβ-II and PKCδ have been implicated in the acute onset of lipid-induced insulin resistance in skeletal muscle (Itani et al., 2002).

Lipid-induced activation of PKCθ promotes the translocation of PKCθ from the cytosol towards the cell membrane where it elicits its effect on the upstream insulin signalling molecules such as the IR and IRS (Ravichandran et al., 2000; Schmitz-Peiffer, 2000; Morino, Petersen, & Shulman, 2006). PKCθ phosphorylates serine (ser) residues on the β-subunit of the IR which prevents phosphorylation of tyrosine residues and subsequent docking of IRS due to conformational changes of the IR (Karasik et al., 1990; Paz et al., 1997; Aguirre et al., 2002; Liu et al., 2004).

There are also over 70 potential serine phosphorylation sites on IRS-1, however only phosphorylation of ser^{302}, ser^{307}, ser^{612}, and ser^{632} have been implicated in insulin resistance in both humans and rodent models (Hirosumi et al., 2002; Kim et al., 2004; Morino et al., 2005; Morino, Petersen, & Shulman, 2006). Likewise, serine phosphorylation of IRS-1 leads to the dissociation of IRS-1 from PI3K, and prevents downstream activation of the insulin signalling pathway (Morino, Petersen, & Shulman, 2006).

Morino et al. (2008) demonstrated that transgenic modification of ser^{302}, ser^{307}, and ser^{612} to alanine residues on IRS-1 in mice defended against diet induced insulin resistance by

maintaining PI3K and Akt activation. This study showcased the crucial role that PKCθ expression and serine phosphorylation of the upstream insulin signalling molecules have on insulin sensitivity and glucose transport.

3.2 Mitochondrial Dysfunction

The accumulation of intramyocellular lipids has previously been suggested to occur due to a decrease in the mitochondria mediated β-oxidation of fatty acids (Morino, Petersen, & Shulman, 2006; Kraegen & Cooney, 2008). Several studies have documented a reduction in mitochondria function following a prolonged high-fat diet (Sparks et al., 2005; Bonnard et al., 2008). Other studies have reported a reduced mitochondria content in skeletal muscle from T2DM patients and their insulin resistant offspring (Petersen et al., 2004; Morino et al., 2005; Ritov et al., 2005). However, these cross-sectional observations of T2DM patients cannot decipher whether the decreased mitochondria content is a cause or consequence of the insulin resistance. Furthermore, more recent observations reveal that insulin resistance is clearly evident prior to a reduction in mitochondrial content (Park et al., 2005; Bonnard et al., 2008).

Turner et al. (2007) have shown that feeding mice a high-fat diet induces the increased expression of several mitochondrial oxidative enzymes and the fatty acid oxidative capacity of the mitochondria. Similarly, Hancock et al. (2008) demonstrated that high-fat feeding in rats produced a gradual increase in skeletal muscle mitochondria content which coincided with the onset of insulin resistance. The increased mitochondrial content was attributed to the observed upregulation of peroxisome proliferator-activated receptor (PPAR)-δ and subsequent increase in PPAR coactivator-1α (PGC-1α) (Hancock et al., 2008). Presumably the increased capacity of the mitochondria for β-oxidation is insufficient to prevent the accumulation of intramuscular lipids.

It is evident that consistency is lacking in regards to the mitochondrial oxidative capacity in models of obesity and insulin resistance (Glatz, Luiken, & Bonen, 2010). Fatty acid oxidation can be either reduced (Bandyopadhyay et al., 2006; Han et al., 2007; Ouwens et al., 2007), unaltered (Young et al., 2002; Smith et al., 2007), or increased (Turcotte et al., 2001; Coort et al., 2004a; Carley & Severson, 2005; Carley et al., 2007) in various rodent models of obesity or insulin resistance. The conflicting evidence in the literature suggests that there are

potentially other contributing factors to the lipid accumulation that is observed in insulin resistance.

3.3 Elevated Free-Fatty Acid Transport in Skeletal Muscle

In healthy individuals, plasma NEFAs are transported into skeletal muscle due to an insulin- or contraction-mediated translocation of fatty acid transporters (CD36) from intracellular depots to the plasma membrane surface (Glatz, Luiken, & Bonen, 2010). Moreover, under basal conditions there is typically a steady distribution of CD36 fatty acid tranporters and GLUT4 transporters embedded in the cell membrane, and stored intracellularly (Glatz, Luiken, & Bonen, 2010).

In models of insulin resistance there is a notable shift in the rate of fatty acid uptake into cardiac and skeletal muscle (Chabowski et al., 2006; Glatz, Luiken, & Bonen, 2010). For instance, the rate of fatty acid transport into skeletal muscle is elevated by 40-80% in both high-fat fed and obese Zucker rats (Luiken et al., 2001; Hegarty et al., 2002) while a 4-fold increase is noted in obese human subjects (Bonen et al., 2004). Interestingly, the increased rate of lipid transport cannot be explained by an upregulation of fatty acid transporter expression as there are no changes in the total content of CD36 or any other fatty acid transport protein in skeletal muscle (Luiken et al., 2001; Han et al., 2007). There is, however, an increase in the number of CD36 transporters located on the plasma membrane in obese skeletal muscle indicating a permanent relocation of the transporters from the intracellular depots to the cell surface (Luiken et al., 2001; Bonen et al., 2004; Han et al., 2007). This increased membrane expression of CD36 highly correlates to the increased rate of fatty acid transport in the skeletal muscle from both obese animal models and human subjects (Bonen et al., 2004; Holloway et al., 2009).

It appears evident that the permanent relocation of CD36 to the plasma membrane has a significant role in the accumulation of intramyocellular lipids and subsequent onset of insulin resistance (Fig. 3.2). The rates of lipid transport, esterification, and oxidation are increased in skeletal muscle from obese Zucker rats (Holloway et al., 2009); however, the rate of esterification was 8-fold greater than that of lipid oxidation when expressed relative to fatty acid transport which indicates the rate of transport exceeds the cell's capacity to oxidize the excess fatty acids (Holloway et al., 2009). Furthermore, directly inhibiting CD36-mediated

fatty acid uptake in insulin resistant tissue from high-fat fed rats and obese Zucker rats lowered the elevated rate of fatty acid esterification (Ploug et al., 1993; Coort et al., 2004a). Also, the elevated CD36-mediated fatty acid uptake has been observed prior to any changes in glucose uptake or onset of insulin resistance in cardiac myocytes from obese Zucker rats (Coort et al., 2004b; Chabowski et al., 2006). Taken together these results support the notion that the accumulation of intramyocellular lipids is attributed to the relocation of CD36 transporters to the plasma membrane and the subsequent increase in fatty acid transport into the skeletal muscle cell.

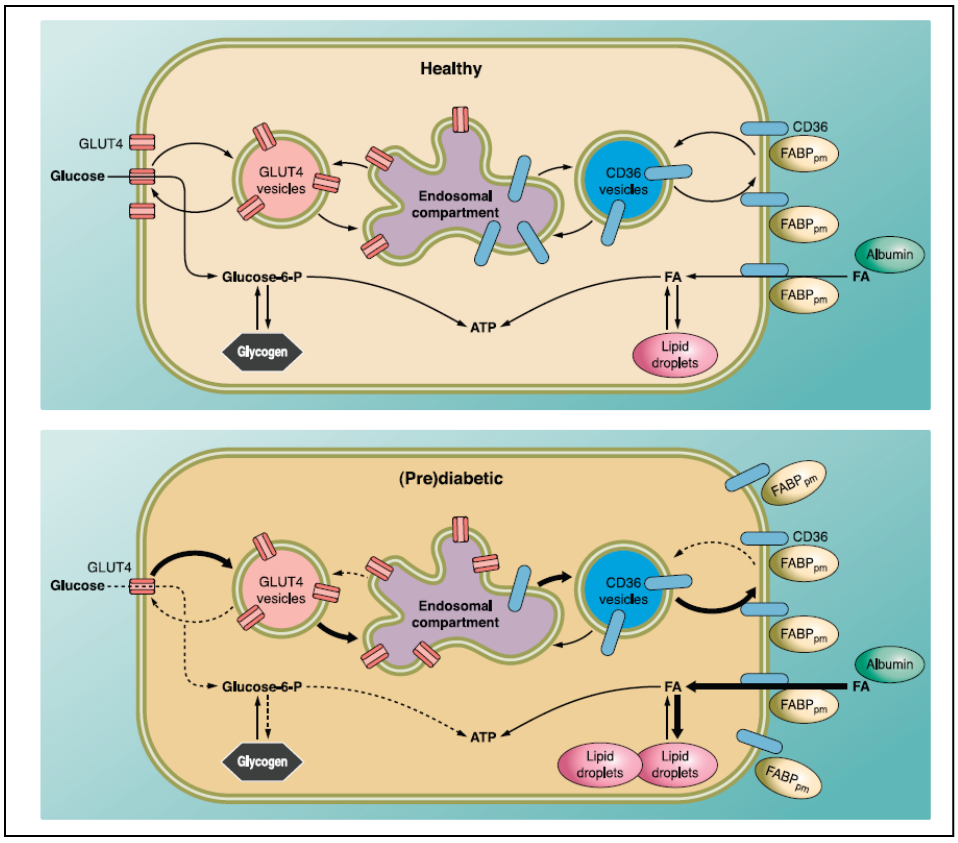

Figure 3.2: Substrate transport in healthy and diabetic individuals. In healthy individuals there is a balance between glucose and NEFA uptake (top). In a diabetic state (bottom) it is proposed that there is an increase in the number of CD36 transporters embedded in the plasma membrane leading to an elevated rate of NEFA transport into the skeletal muscle cell (Glatz, Luiken, & Bonen, 2010).

4.0 Rodent Obesity and Diabetes Models

The study of the progression of diabetes has been propelled over the past quarter of a century thanks in part to the discovery of several experimental rodent models that spontaneously portray common characteristics observed in human diabetes mellitus patients. Most notably the Otsuka Long-Evans Tokushima fatty rats, ob/ob mice, db/db mice, and Zucker Diabetic fatty rats exhibit moderate to severe obesity, hyperglycaemia, hyperinsulinemia, insulin resistance, deficient glucose stimulated insulin secretion, and reduced glucose transporter translocation in a comparable disease progression as in humans (Dubuc, 1976, Coleman, 1980; Coleman, 1982; Kawano et al., 1992; Kawano et al., 1994; Etgen & Oldham, 2000; Chen & Wang, 2005). However, these rodent models are not without limitations. For instance, one drawback of the ob/ob mouse is that the mutation of the leptin gene and subsequent lack of leptin production is not representative of the disease in the majority of humans since humans typically are hyperleptinemic and leptin resistant (Baribault, 2010). Diet-induced obesity in the C57BL/6J mouse strain is another common model that produces an intermediate susceptibility to diabetes-related symptoms such as hyperglycemia, hyperinsulemia, and fatty liver; however, the later stages of the disease such as pancreatic islet destruction and diabetic nephropathy are rarely seen (Baribault, 2010).

5.0 Introduction to Sarcolipin

5.1 Sarcolipin Mouse Model

A potential novel mouse model for obesity and diabetes mellitus has been proposed by our laboratory (Sayer et al., 2008). The sarcolipin (SLN) knockout mouse (Babu et al., 2007a) has been shown to significantly gain more weight and adiposity than littermate control mice following an 8-week high fat diet (Sayer et al., 2008). Further, the KO mice became hyperglycaemic and hyperinsulinemic, and have elevated plasma levels of leptin, non-esterfied fatty acids, and cholesterol (Bal et al., 2009). Both the KO and the wild-type control groups displayed glucose intolerance and insulin resistance following the high-fat diet intervention; however, surprisingly the KO mice exhibited a more severely impaired response to glucose than the control mice during a 2-hour glucose tolerance test; however, HFD fed KO mice exhibited a comparable reduction in insulin sensitivity as HFD fed controls (Sayer et al., 2008; Bal et al., 2009). The KO mouse model appears to follow the usual disease progression of type II diabetes mellitus as all of these symptoms are typically associated with the disease (Reaven, 1995; Alberti & Zimmet, 1998; Baribault, 2010). However, the origin of the glucose intolerance is currently unknown as SLN is not proposed to directly influence glucose uptake.

5.2 Role of Sarcolipin in Skeletal Muscle

SLN is a 31-amino acid integral membrane protein that is found in abundance in the atria and moderately in slow-twitch musculature, such as the diaphragm or soleus muscle, in rodent tissue (Babu et al., 2007b). In larger mammals, such as rabbits and dogs, SLN protein levels are greater in both slow and fast twitch muscle compared to levels observed in the atria suggesting that SLN may assert a more significant role in skeletal muscle function in larger mammals (Babu et al., 2007b).

SLN is closely associated with the sarco/endoplasmic reticulum calcium-ATPase (SERCA) within the sarcoplasmic reticulum membrane of atria and skeletal muscle cells (Wawrzynow et al., 1992; Asahi et al., 2002; Babu et al., 2007b). SERCA proteins (110 kDa) are well known Ca^{2+} pumps that transport Ca^{2+} ions across a membrane against a gradient ($>10^4$-fold) in response to ATP hydrolysis thereby maintaining the basal cytosolic Ca^{2+} concentration in skeletal muscle near 100 nM (Toyoshima, 2008). During repetitive exercise (i.e. muscle contractions) SERCA rapidly resequesters large amounts of Ca^{2+} into the SR

(Tupling, 2004). This process is imperative to the contraction-relaxation cycle of repetitive exercise.

The Ca^{2+} transport ability of SERCA is regulated by SLN through a physical interaction between the two membrane-bound proteins (Asahi et al., 2002; Asahi et al., 2003). Asahi et al. (2002) have shown that the co-expression of SERCA and SLN reduces the Ca^{2+}-dependent Ca^{2+} transport of both primary skeletal muscle isoforms of SERCA (1a and 2a) at all Ca^{2+} concentrations under physiological conditions in HEK-293 cells as indicated from the rightward shift of the calcium concentration curve in Figure 5.1. Despite the decreased accumulation of Ca^{2+} in reconstituted SR vesicles, the presence of SLN has no effect on the rate of Ca^{2+}-ATPase activity (Smith et al., 2002). Similarly, analyses of isolated soleus muscles from KO mice have also revealed that SLN uncouples ATP hydrolysis from Ca^{2+} transport (Bombardier et al., 2008).

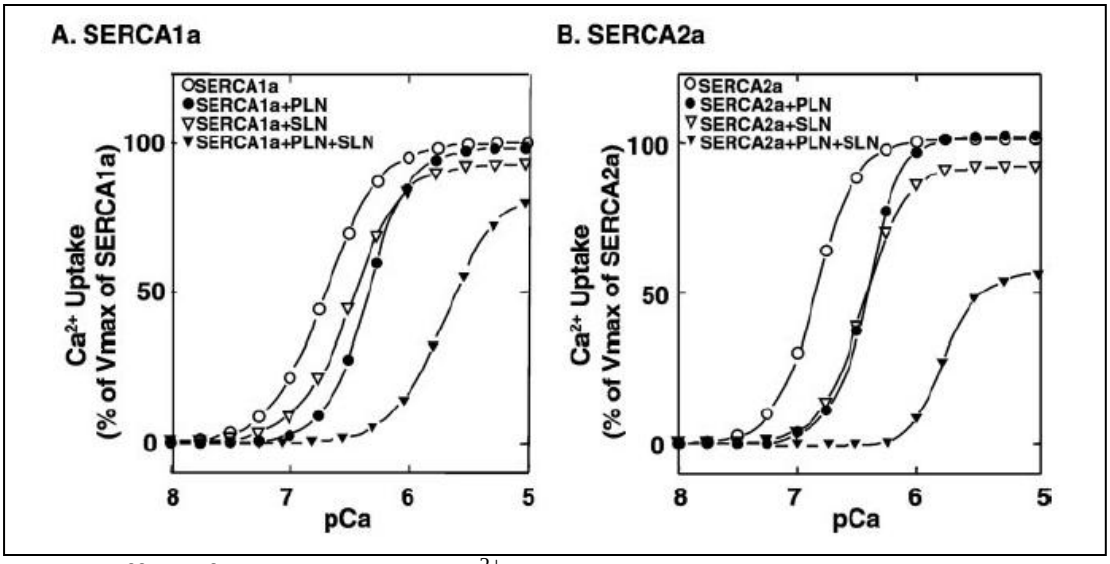

Figure 5.1: Effect of SLN on SERCA Ca^{2+} Uptake (Asahi et al., 2002)

5.3 Sarcolipin and Disease

It is speculated that the diet-induced glucose intolerance observed in the KO mice develops as an indirect consequence of a chronic positive energy imbalance and the development of obesity. SERCA accounts for approximately 50% of the resting energy requirements of skeletal muscle (Norris et al., 2009) which suggests that SERCA has a significant role in daily whole body energy expenditure (Zurlo et al., 1990; Rolfe & Brown, 1997; Levine, 2003). Not surprisingly, lowering the efficiency of the SERCA pump in soleus muscle through the uncoupling activity of SLN results in a 10% greater energy consumption of SERCA in wildtype muscle compared to KO muscle (unpublished results). Even a small variation in total daily whole body energy expenditure, such as altering the contribution of SERCA, can impose serious consequences on weight gain and health indicators as evidenced by the KO mouse model (Sayer et al., 2008; Bal et al., 2009; Butler & Kozak, 2010).

6.0 Purpose of Study

6.1 Rationale for Study

The purpose of this study is to examine the effects of high fat feeding on the insulin signalling cascade in skeletal muscle from KO mice. As noted previously, after completion of an 8-week high-fat diet intervention, the KO mice become more obese and have more pronounced glucose intolerance than wild-type littermates (Sayer et al., 2008; Bal et al., 2009). However, the mechanisms involved remain to be established.

Insulin resistance is a common feature of diet-induced obesity (Shulman, 2000; Morino, Petersen, & Shulman, 2006). Moreover, results from whole body glucose tolerance testing generally correlate well with the results from the euglycemic-hyperinsulinemic clamp technique (Bergman et al., 1987; Bergman, 1989), which is the gold standard for the assessment of insulin resistance (DeFronzo, Tobin, & Andres, 1979). Therefore, it is reasonable to expect that the KO mice would exhibit a noticeably greater degree of peripheral insulin resistance. As previously discussed, insulin resistance is the result of an insufficient insulin-stimulated glucose uptake (Timmers, Schrauwen, & de Vogel, 2007). Generally, a breakdown in the insulin signalling cascade is the primary reason for the decreased glucose transport in models of diet-induced obesity and diabetes. Thus, this study examined the extent of diet-induced impairment of the insulin signalling cascade in the KO mice. More specifically, IRS1 tyr^{628} and Akt ser^{473} phosphorylation will be assessed as markers for the degree of insulin signalling pathway activation as previous described (Fujii et al., 2004; Morino et al., 2008; Mullen et al., 2009). Further, changes in IRS1 ser^{307} phosphorylation will be examined in an attempt to characterize a plausible mechanism for potential post-HFD decreases in IRS1 activation. The information provided from this study will help to characterize the KO mouse as a potential model of severe diet-induced obesity and diabetes.

6.2 Brief Description of Experimental Approach

The euglycemic-hyperinsulinemic clamp is the most accurate method to assess insulin resistance quantitatively (DeFronzo, Tobin, & Andres, 1979). However, it is quite difficult to perform in mice, and has a high associated cost to perform the testing procedure. This study proposed to assess the insulin signalling pathway in skeletal muscle through the analysis of

several key phosphorylation sites on signalling proteins of the insulin cascade of glucose uptake. Numerous studies have utilized antibodies for the specific phosphorylation sites and to quantify the amount of each protein by Western blot techniques (Fujii et al., 2004; Morino et al., 2008; Mullen et al., 2009).

6.3 Specific Objectives

There are several key objectives associated with the present investigation. The goal(s) of the study were to:

a) Assess the effects of an 8-week high-fat diet on whole body and fat pad weight(s) in KO and wildtype mice;
b) Evaluate potential differences in the glucose handling capability of the KO and wildtype mice by means of a 2-hour glucose tolerance test following the high-fat diet intervention;
c) Utilize an intraperitoneal insulin bolus to examine the insulin sensitivity of both mouse genotypes during a 2-hour insulin tolerance test;
d) Examine the effects of SLN ablation on insulin-stimulated tyr^{628} phosphorylation of IRS1 and ser^{473} phosphorylation of Akt following the high-fat diet;
e) Compare the degree of ser^{307} phosphorylation of IRS1 after the completion of the high-fat diet in KO and wildtype mice.

6.4 Hypotheses

Following the 8-week high-fat diet the KO mice will:

a) Gain more weight and become more obese compared to control mice;
b) Exhibit a greater intolerance to glucose compared to control mice as assessed by a glucose tolerance test;
c) Show no significant differences in whole body insulin sensitivity compared to control mice fed the high-fat diet as assessed by an insulin tolerance test;
d) Demonstrate a significant reduction of insulin-stimulated tyr^{628} phosphorylation of IRS1 and ser^{473} phosphorylation of Akt compared to control mice;
e) Display a greater level of ser^{307} phosphorylation of the IRS1 molecule compared to littermate control mice.

7.0 METHODS

7.1 Animal Colonies

A sarcolipin knockout mouse model (KO) was donated by Dr. Muthu Periasamy from Ohio State University to establish a viable mouse colony. Breeding pairs for the colony were born from cross-breeding KO mice with C57BL mice, thus generating heterozygous KO mice. The heterozygous KO mice were bred producing homozygous wild type (WT, +/+), heterozygous (HET, +/-), and homozygous-null (KO, -/-) mice.

Genotyping of mice was performed on extracted DNA from 4 week old mice using a Genomic DNA mini kit (Invitrogen). The DNA of interest was amplified by RT-PCR and imaged using a bio-imaging system (Syngene). Briefly, 50 ng of extracted DNA was added to a Taq DNA polymerase mix (Fermentas: 3mM $MgCl_2$, 200 µM dNTP, & 1u of Taq DNA polymerase) and 0.4 µM each of the appropriate 5' and 3' genomic primers (SLN-WT, forward, 5'-TGT CCT CAT CAC CGT TCT CCT-3'and reverse 5'-GCT GGA GCA TCT TGG CTA ATC-3'; KO, Forward, 5'- GTG GCC AGA GCT TTC CAA TA-3'and reverse 5'-CAA AAC CAA ATT AAG GGC CA-3'). Samples were placed in a thermal cycler (MJ MINI, BIO-RAD) and denatured for 3 minutes at 94°C followed by 30 cycles of denaturation for 30 sec at 94°C, annealing for 30 sec at 54°C, and extension for 60 sec at 72°C, this followed by a final extension at 72°C for 7 min. The amplified products were then separated on a 1% agrose gel containing 0.01% ethidium bromide (BioShop) and identified using a bio-imaging system and densitometric analysis which was performed using the GeneSnap software (Syngene).

7.2 Experimental Protocol

Fifty-four age-matched animals (27 WT; 27 KO) were individually housed in an environmentally controlled room on a 12:12hr light/dark cycle for the duration of the twelve week study period. Prior to the intervention period all of the experimental animals were fed a standard chow diet (60% of calories from carbohydrate, 5% of calories from fat; Tekland 22/5 Rodent Diet, Harland-Tekland, Madison, WI) and water ad libitum. Further, all animals underwent glucose and insulin tolerance tests (details to follow) prior to the start of the diet intervention.

At approximately 16 weeks of age the animals were sub-divided into two groups where one group was fed a high-fat diet (42% of calories from fat; product TD 88137, Harlan Teklad, Madison, WI) for an eight week intervention period while a control diet group remained on the chow food. Body weight was measured prior to the intervention and subsequent changes in mass were assessed on a weekly basis. Following the 8-week diet intervention, glucose and insulin tolerance tests were reassessed. The mice were sacrificed and tissue was collected one week after the final insulin tolerance test. Please refer to Figures 7.1 and 7.2 for experimental design details, and Appendices A and B for detailed diet information.

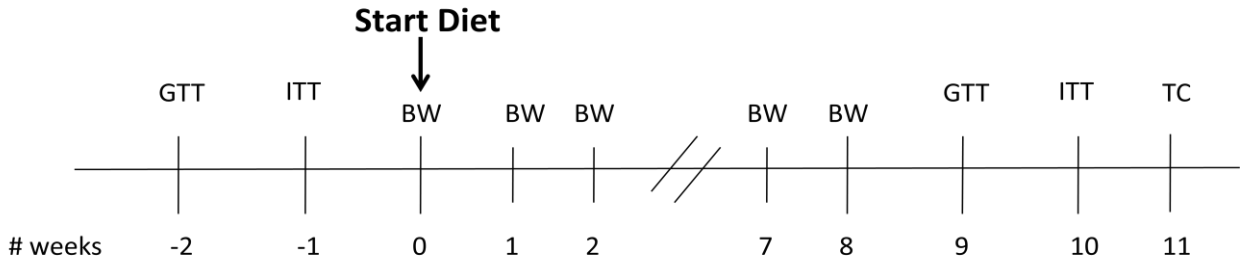

Figure 7.1: Experimental Study Timeline (GTT: glucose tolerance test; ITT: insulin tolerance test; BW: body weight measurement; TC: tissue collection)

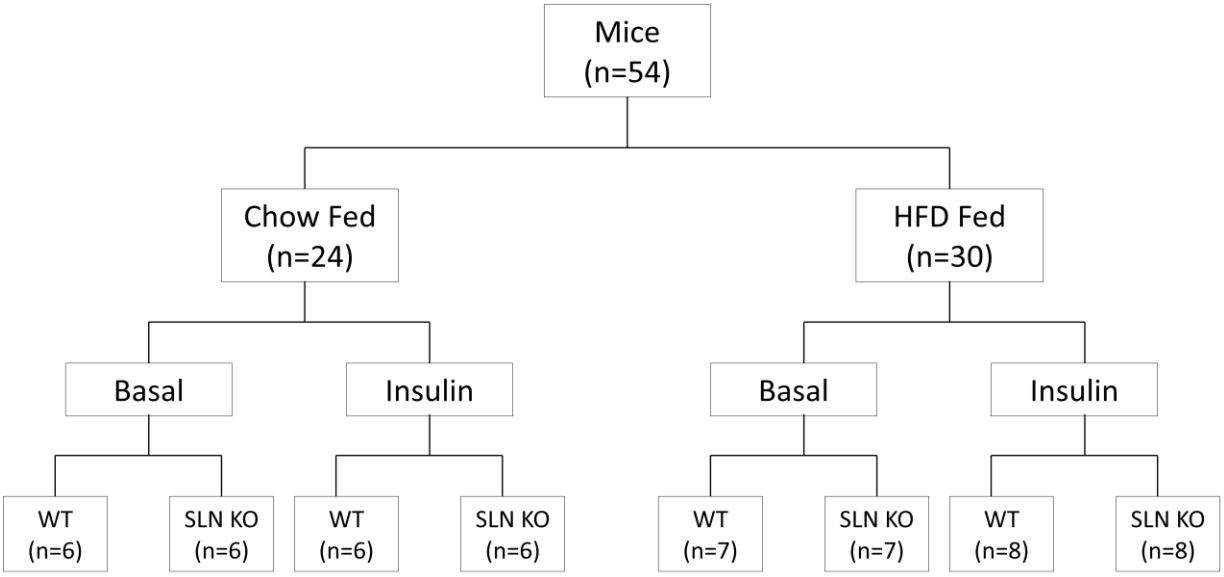

Figure 7.2: Experimental Study Design (HFD: high-fat diet; basal: vehicle injection pre-tissue collection; insulin: intraperitoneal injection of insulin pre-tissue collection; WT: wild-type mice; SLN KO: sarcolipin-null mice)

7.3 Glucose and Insulin Tolerance Tests

Glucose tolerance testing was performed following an overnight fast (16 hours) for both high-fat and chow fed animals. Venous blood samples (6 μL) were drawn from the tail and assessed for glucose using a blood glucometer (Accu-Chek Aviva, Roche Diagnostics) at 0, 30, 60, and 120 minutes following a 1g/kg body weight intraperitoneal injection of 10% D-glucose (Li et al., 2000).

Insulin tolerance testing was performed on both high-fat and chow fed animals one-week following the glucose tolerance test. The animals were fasted for 4-hours prior to an intraperitoneal injection of insulin (Humulin, Eli Lilly, Toronto, CA) at a dose of 0.75U/kg body weight. Blood samples were drawn from the tail and assessed for glucose using a blood glucometer (Accu-Chek Aviva, Roche Diagnostics) at 0, 30, 60, and 120 minutes post injection (Li et al., 2000).

7.4 Tissue Collection

Upon completion of the 8-week high fat diet, the phosphorylation state of several key insulin signalling molecules in skeletal muscle was assessed as previously described (Fujii et al., 2004; Morino et al., 2008). Fasted (4-hours) KO mice and wildtype littermates (HFD and chow-fed mice) were anaesthetized using sodium pentobarbital (0.65 mg/kg body weight) and were subjected to an intraperitoneal injection of insulin (0.75 units/kg) or vehicle solution (Fig. 7.2). Whole gastrocnemius muscle was excised from each leg 15-min post-injection and freeze clamped immediately using aluminum tongs pre-cooled in liquid nitrogen. Tissue samples were stored at -80^{o}C until further analysis. Next, the epididymal/inguinal and retroperitoneal fat pads were surgically removed for determination of the adiposity index.

7.5 Adiposity Index Calculation

The adiposity index was defined as the percentage that the epididymal/inguinal and retroperitoneal fat pads accounted for in relation to total body mass. The adiposity index was calculated as (Taylor and Phillips, 1996):

1) Adiposity Index (%) = (sum of the fat pad masses) / body mass * 100

7.6 Skeletal Muscle Homogenization

Frozen tissue samples (100 mg) were homogenized in a buffer consisting of (mM): 50 Tris-HCl, 1 EGTA, 1 EDTA, 1% Triton X-100, 50 NaF, 5 sodium pyrophosphate, 10 sodium β-glycerol phosphate, 2 DTT, 1 sodium orthovanadate , 1 PMSF, and 10 μg/mL each of aprotinin, leupeptin, and pepstatin A. Protein content for each sample was determined using the Lowry protein method, as modified by Schacterle and Pollock (Schacterle & Pollock, 1973).

7.7 Immunoblotting

Muscle homogenate (IRS1 antibodies: 25 μg; phosphor-IRS1 antibodies: 30 μg; Akt antibodies: 6 μg) was separated by SDS-PAGE protocols (Laemmli, 1970) and transferred to polyvinylidene fluoride membranes (Roche Diagnostics, Mannheim, Germany). The polyvinylidene fluoride membranes were blocked for 1 hour at room temperature in Tris-buffered saline with a 5% skim milk suspension, and subsequently incubated overnight at 4^{o}C with antibodies for total (anti-IRS1 clone 4.2.2; Millipore), phospho-Tyr^{628} (anti-phospho-IRS1 Tyr^{628}; Millipore), and phospho-Ser^{307} (anti-phospho-IRS1 Ser^{307} clone 24.6.2; Millipore) IRS-1, and total (anti-Akt 5G3; Cell Signaling) and phospho-Ser^{473} (anti-phospho-Akt Ser^{473} 587F11; Cell Signaling) Akt. After washing, the membranes were incubated with horseradish peroxidise-conjugated anti-mouse or anti-rabbit secondary antibody (Santa Cruz Biotechnology) for 1 hour at room temperature. The blots were detected with an enhanced chemiluminescence kit (Amersham Pharmacia Biotech) using a bio-imaging system and densitometric analysis performed using the GeneSnap software (Syngene). Densitometric analysis was normalized to a control sample that was loaded onto each individual membrane to account for inter-membrane variability.

7.8 Statistical Analysis

Two-way ANOVAs were used to assess differences in body weight, fat pad weight, and the adiposity index between KO and WT mice in both HFD and chow-fed groups. Three-way ANOVAs were utilized to investigate differences in phosphorylation states of IRS1 and Akt from Western blot analysis between KO and WT mice in both diet groups. Furthermore, three-way ANOVAs with repeated measures were used to detect differences between the glucose and insulin tolerance test data of KO and WT mice at pre- and post-diet time points for different

times (0, 30, 60 and 120 min) for both diet groups. The significance level was set at 0.05, and when appropriate, a Newman-Keuls post hoc test was used to compare specific means. Trends in results will be mentioned when the significance value is less than 0.15. All values are reported as means ± standard error (SE). Sample sizes for the body and fat pad weight(s), adiposity index, and glucose and insulin tolerance test reflect the total number of mice in the chow fed or high fat fed groups (Fig. 7.2).

8.0 RESULTS

8.1 Body Weight

Prior to the HFD, there were no differences in body weight (Fig. 8.1) between KO and WT mice ($p>0.05$). Moreover, no significant weight gain was observed in chow fed mice throughout the study ($p>0.05$). The HFD fed KO mice weighed significantly more than HFD fed WT mice at all time points during the 8-week period ($p<0.001$). Similarly, the HFD fed KO mice weighed significantly more than the standard chow fed control mice at all time points ($p<0.001$). The HFD fed WT mice weighed significantly more than chow fed WT mice at all time points following week 1 ($p<0.01$).

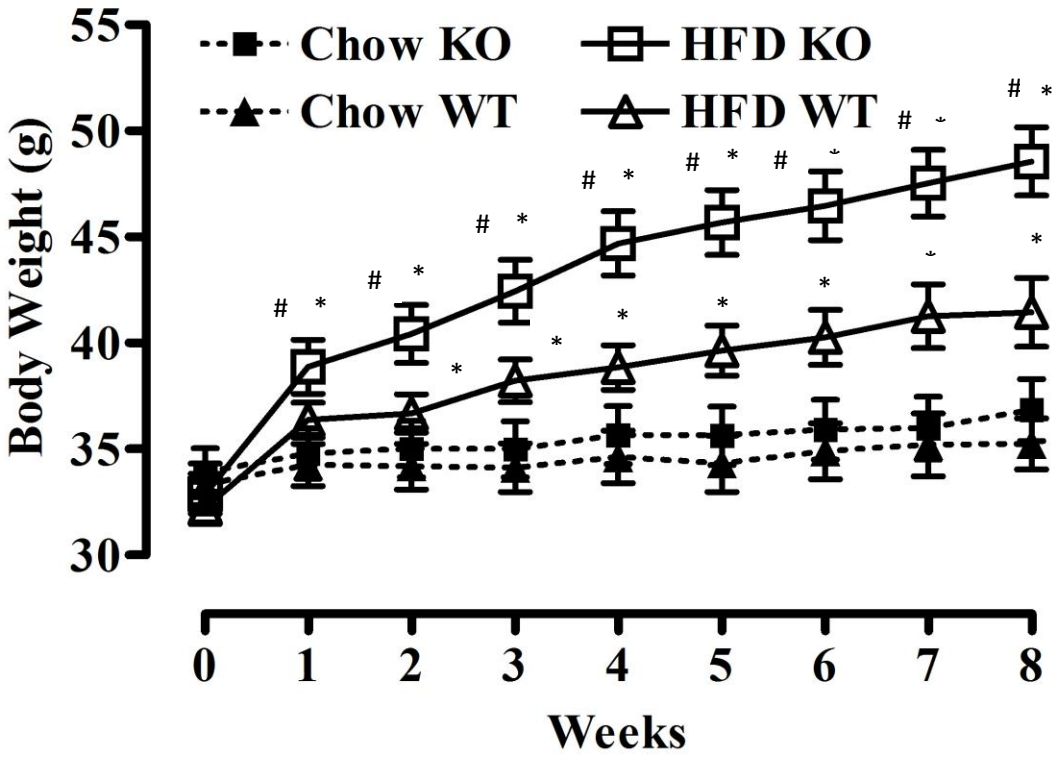

Figure 8.1. Absolute Change in Body Weight during the course of the 8-week high-fat or chow-diet intervention. There was no difference between KO and WT mice pre-diet ($p>0.05$). There was no significant difference between post-diet chow-fed KO and WT mice. HFD fed KO and WT mice weighed significantly more than control mice (* $p<0.01$). Further, HFD fed KO weighed significantly more than HFD fed WT (# $p<0.001$). Values are means ± SE (n=12 for WT and KO control; n=15 for WT and KO HFD).

8.2 Adiposity Measures

Ex vivo measures for differences in adiposity revealed a main effect in which KO mice had a significantly larger epididymal/inguinal fat pad weight than WT mice irrespective of diet (Fig. 8.2A) ($p<0.05$). Further, a main effect was observed where HFD fed mice (KO and WT combined) had a significantly greater epididymal/inguinal fat pad weight than standard chow fed mice ($p<0.0001$). It was also observed that the HFD fed KO and WT mice had significantly greater retroperitoneal fat pad weights (Fig. 8.2B) than their respective chow fed control mice ($p<0.01$). However, the HFD fed KO mice had a significantly greater retroperitoneal fat pad weight than the HFD WT mice ($p<0.001$). The calculation of the adiposity index (Fig. 8.3) revealed a main effect of genotype (KO > WT; $p<0.05$) and a main effect of diet (HFD > Chow; $p<0.0001$). There was no difference between chow fed KO and WT mice in epididymal/inguinal or retroperitoneal fat pad weights, or adiposity index ($p>0.05$). Adiposity index values for all mice were in line with previous reports regardless of diet (Taylor & Phillips, 1996).

8.3 Glucose Tolerance Testing

Glucose tolerance testing of the standard chow fed mice showed no significant difference in plasma glucose measures at any time point tested (0, 30, 60, or 120 min) between KO and WT mice either pre or post the 8-week diet time period (Fig. 8.4; $p>0.05$). However, there was a main effect observed where post-HFD fed mice (Fig. 8.5) had elevated plasma glucose measures at all time points compared with pre-HFD fed mice ($p<0.001$). Additionally, post-HFD fed KO mice exhibited significantly higher plasma glucose levels at 30, 60, and 120 minutes post glucose injection than post-HFD fed WT mice ($p<0.001$). Intraperitoneal injection of glucose caused a significant increase in plasma glucose concentration in both pre-HFD and chow fed KO and WT (0 min<60<30; $p<0.001$), and post-HFD KO and WT mice (0 min<120<60<30; $p<0.001$).

A

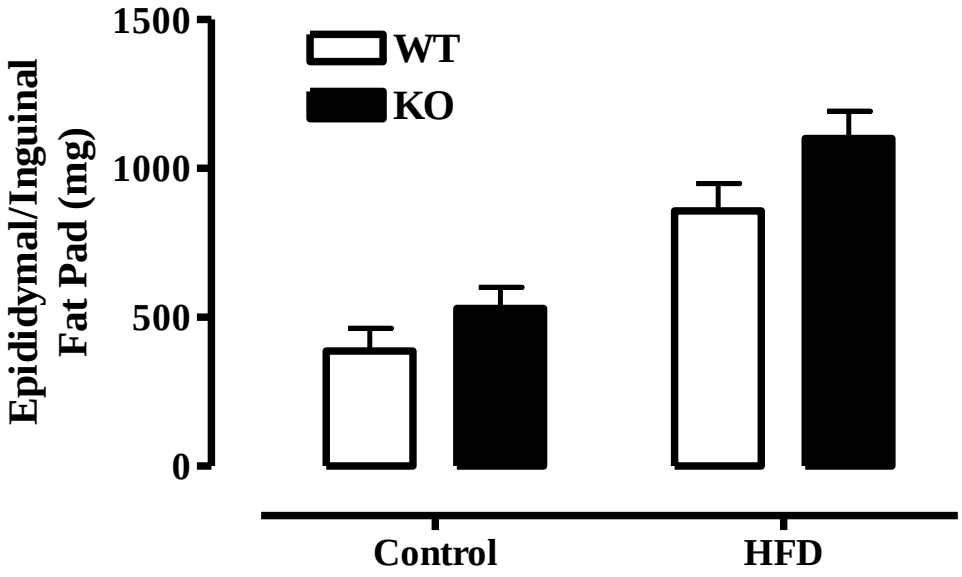

B

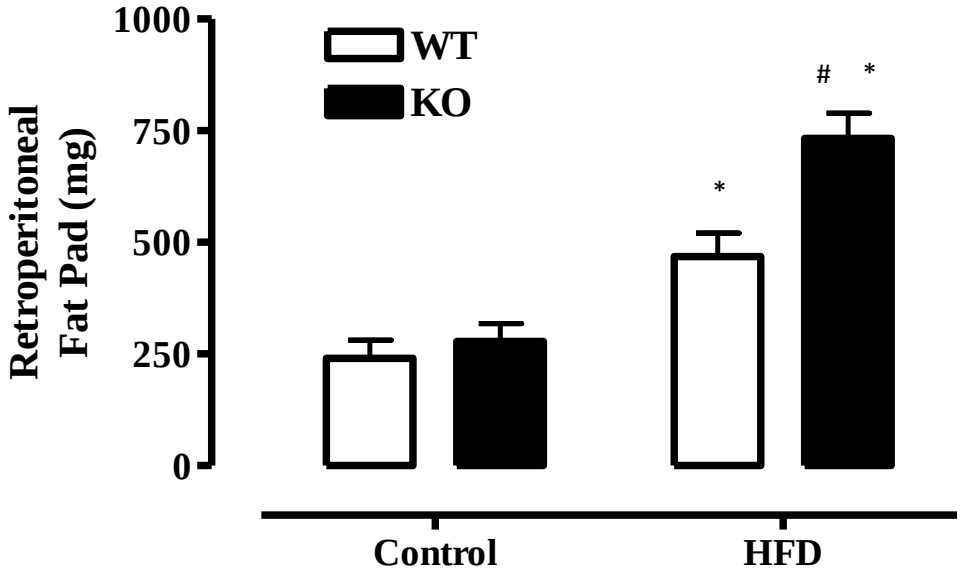

Figure 8.2. Adiposity measures for chow and HFD fed mice. (A) epididymal and inguinal fat pad weight; (B) retroperitoneal fat pad weight. (A) There is a main effect of genotype (KO > WT; $p<0.05$) and of diet (HFD > Chow; $p<0.001$). (B) * Significantly different than control ($p<0.01$). # Significantly different than HFD WT ($p<0.001$). Values are means ± SE (n=12 for WT and KO control; n=15 for WT and KO HFD).

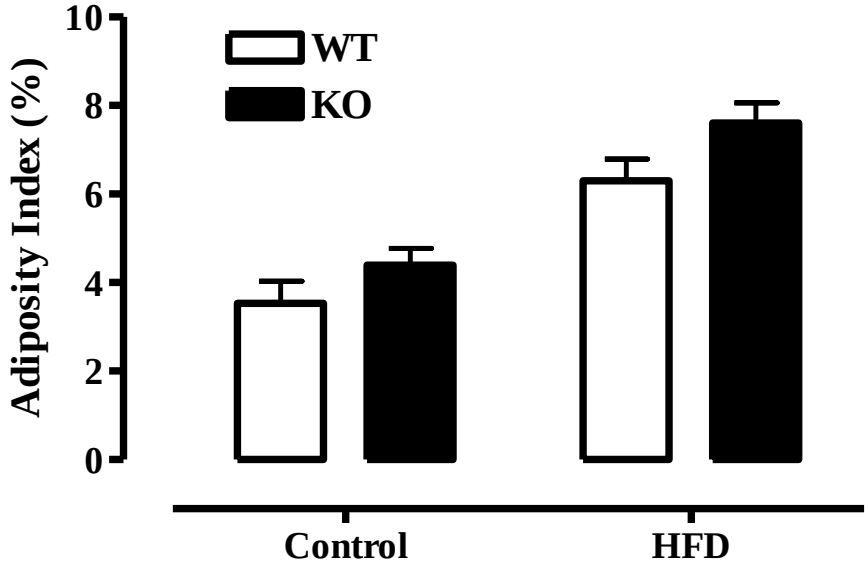

Figure 8.3. Adiposity Index for chow and HFD fed mice. There is a main effect of genotype (KO > WT; $p<0.05$) and of diet (HFD > Chow; $p<0.001$). Values are means ± SE (n=12 for WT and KO control; n=15 for WT and KO HFD).

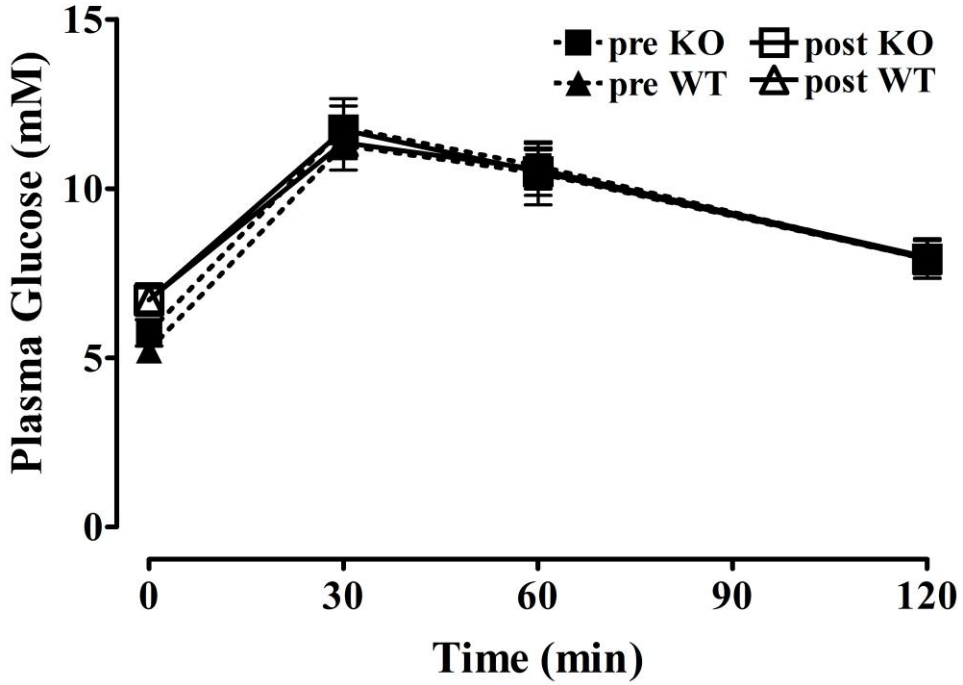

Figure 8.4. Glucose tolerance test pre and post chow diet. There was a main effect of time ($0<60<30$ min; $p<0.001$). There were no significant differences observed in plasma glucose levels between pre- and post-chow fed mice, or SLN KO and WT mice ($p>0.05$). Values are means ± SE (n=12).

8.4 Insulin Tolerance Testing

There was a main effect of age noted in which the post-chow fed mice (KO and WT combined) had on average a greater absolute plasma glucose concentration (Fig. 8.6A) than pre-diet period mice ($p<0.01$). Nonetheless, there were no notable differences in absolute or relative (Fig. 8.6B) plasma glucose measures at any time point (0, 30, 60, or 120 minutes) during the insulin tolerance test between the standard chow fed KO or WT mice either pre- or post-diet period ($p>0.05$). There was no significant difference between KO and WT pre- or post-diet in the area under the curve (AUC; Fig. 8.7) for the absolute change in plasma glucose concentration during the insulin tolerance test ($p>0.05$). There was a main effect of time (0<30, 60, and 120 min) following insulin injection ($p<0.001$).

The HFD intervention resulted in a greater absolute fasting plasma glucose measure (Fig. 8.8A) for both post-HFD fed KO and WT mice compared to pre-HFD fed controls ($p<0.001$). Similarly, there was a main effect where on average the HFD fed mice (KO and WT combined) had an elevated absolute plasma glucose level during the course of the test than pre-HFD and standard chow fed control mice (Fig. 8.8A; $p<0.001$). Additionally, the HFD elicited a main effect where the HFD-fed mice (KO and WT combined) had a lower relative change in the plasma glucose concentration (Fig. 8.8B) 30-minutes post-insulin compared to pre-HFD control mice ($p<0.01$). Interestingly, on average there was a higher plasma glucose concentration observed for the KO mice than the WT mice regardless of diet (Fig. 8.8A; $p<0.05$). However, there were no significant differences between KO and WT mice in the absolute or relative change of plasma glucose at any individual time point during the insulin tolerance test pre- or post-HFD ($p>0.05$). As seen with the chow fed mice, there were no significant differences between KO and WT pre- or post-diet in the AUC (Fig. 8.9) for the absolute change in plasma glucose concentration during the insulin tolerance test ($p>0.05$). There was a main effect of time (0<30, 60, and 120 min) following insulin injection ($p<0.001$).

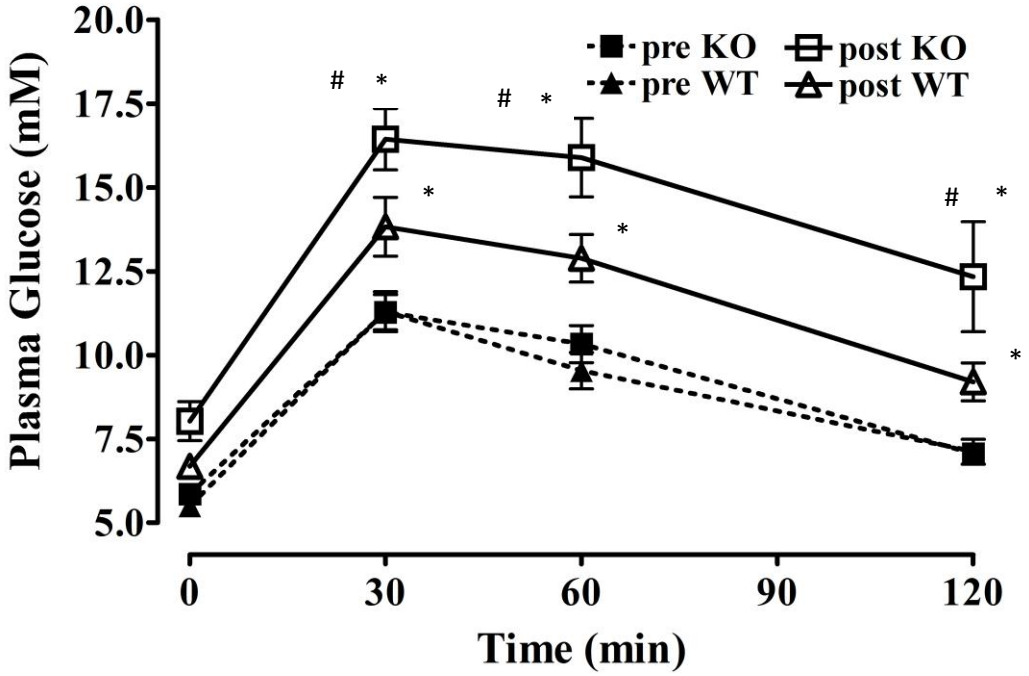

Figure 8.5. Glucose tolerance test pre and post high fat diet. There was a main effect of time (pre: 0<60<30 min; post: 0<120<60<30 min; $p<0.001$). High-fat fed mice had significantly greater plasma glucose levels at 30, 60, and 120 min than pre-diet mice (* $p<0.001$). HFD KO mice had greater plasma glucose levels at 30, 60, and 120 min than HFD WT mice following an intraperitoneal injection of glucose (# $p<0.01$). Values are means ± SE (n=15).

A

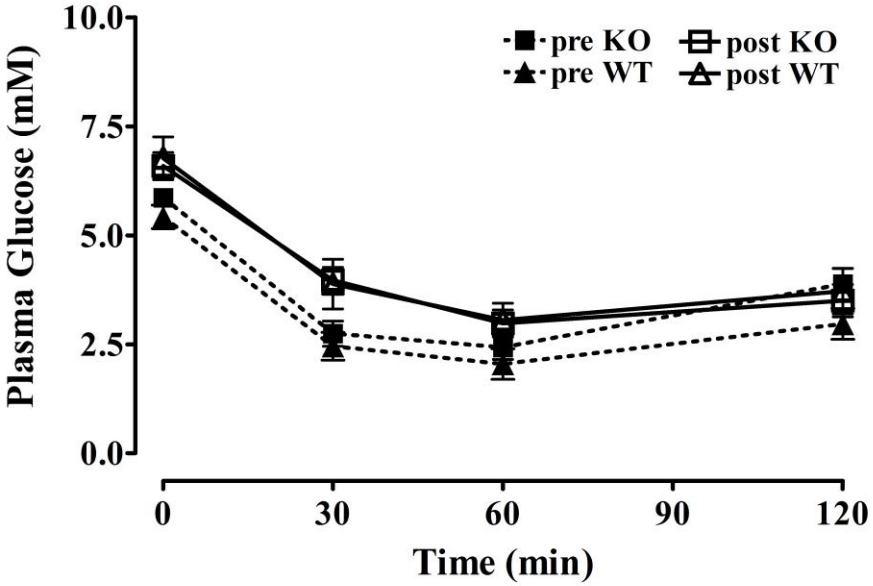

B

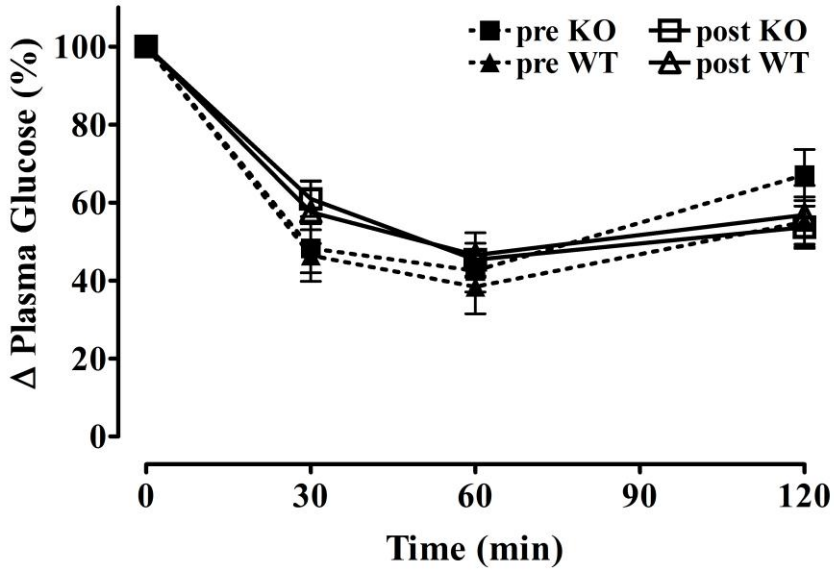

Figure 8.6. Insulin tolerance test pre- and post-chow diet. (A) absolute plasma glucose measure; (B) relative change in plasma glucose. A main effect was observed where post-diet mice had an elevated absolute plasma glucose measure on average compared to pre-diet mice ($p<0.01$). No significant difference KO versus WT ($p>0.05$). Main effect of time ($0 <$ 30, 60, & 120 min; $p<0.001$). Values are means ± SE ($n=9$).

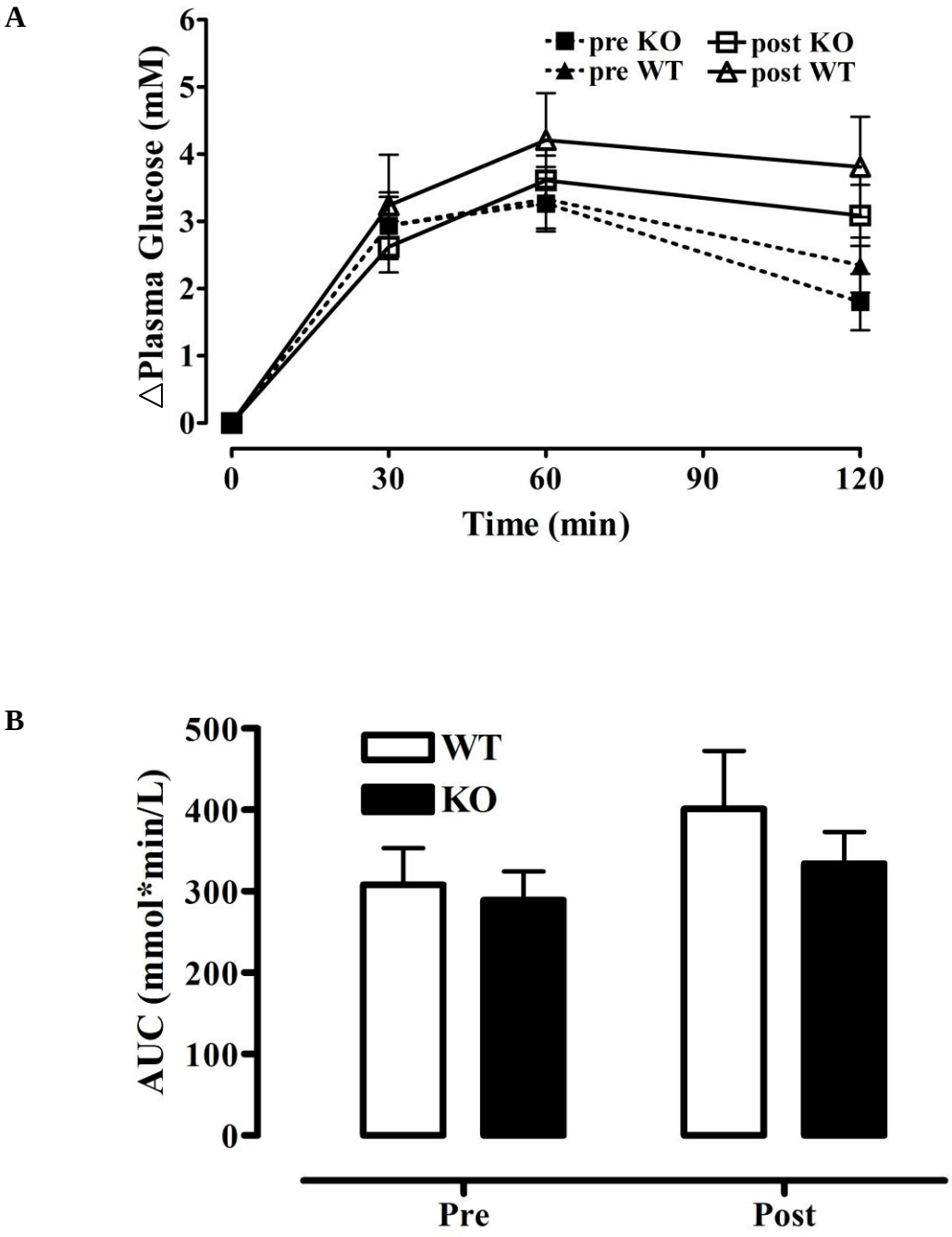

Figure 8.7. AUC for the insulin tolerance test pre- and post-chow diet. (A) absolute change in plasma glucose; (B) area under the curve (AUC). There were no significant differences observed in AUC between KO and WT mice pre- or post-chow diet ($p>0.05$). Values are means ± SE (n=9).

A

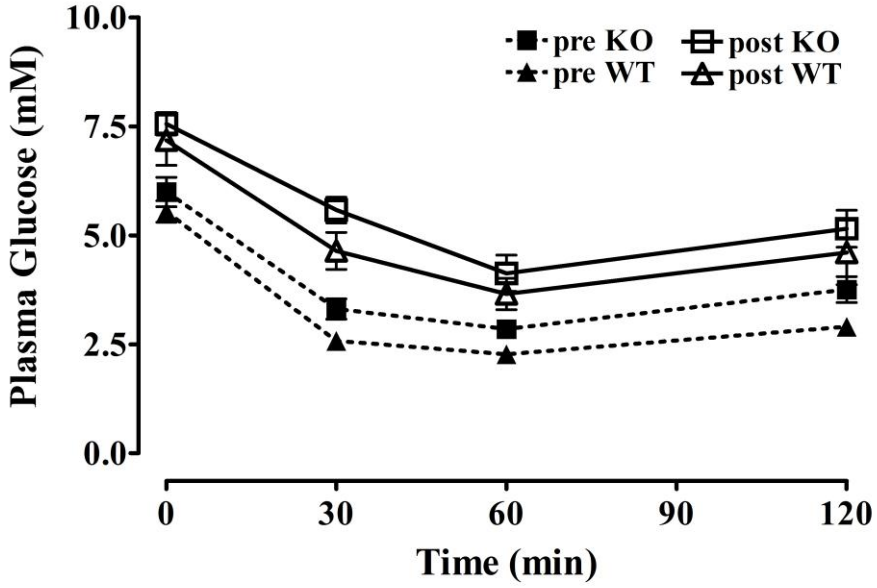

B

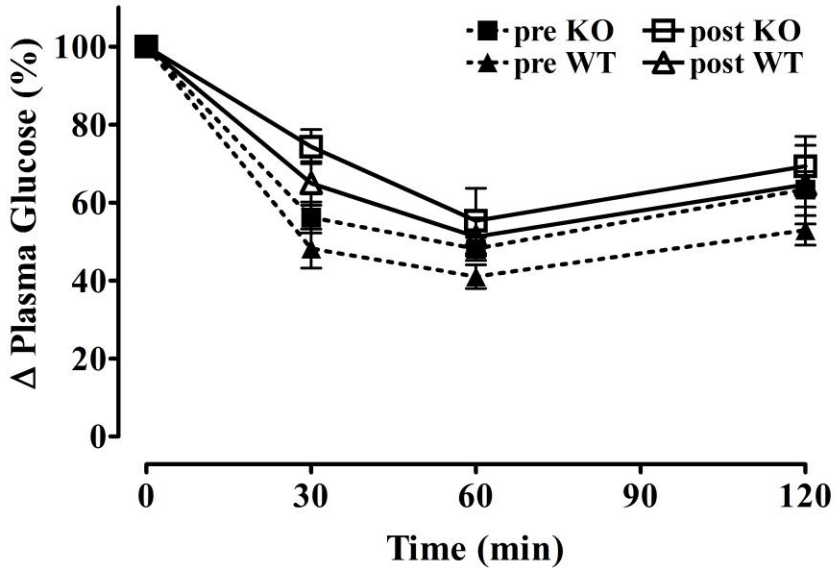

Figure 8.8. Insulin tolerance test pre- and post-HFD. (A) absolute plasma glucose measure; (B) relative change in plasma glucose. (A) Fasting glucose was greater post-HFD (post KO > pre KO; post WT > pre WT) than pre-diet controls ($p<0.001$). There was a main effect of genotype (KO > WT; $p<0.05$) and of diet (HFD > Control; $p<0.001$). (B) There was a main effect of diet (HFD > Control; $p<0.01$) at the 30-min time point. There were no significant differences observed in plasma glucose levels (A) or (B) between KO and WT mice pre- or post-chow diet ($p>0.05$). Main effect of time (0 < 30, 60, & 120 min; $p<0.001$). Values are means ± SE (n=13).

A

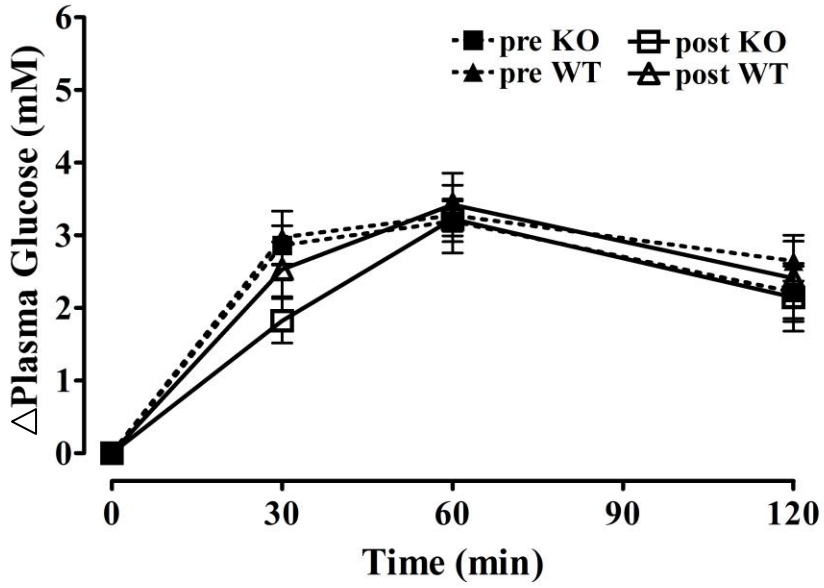

B

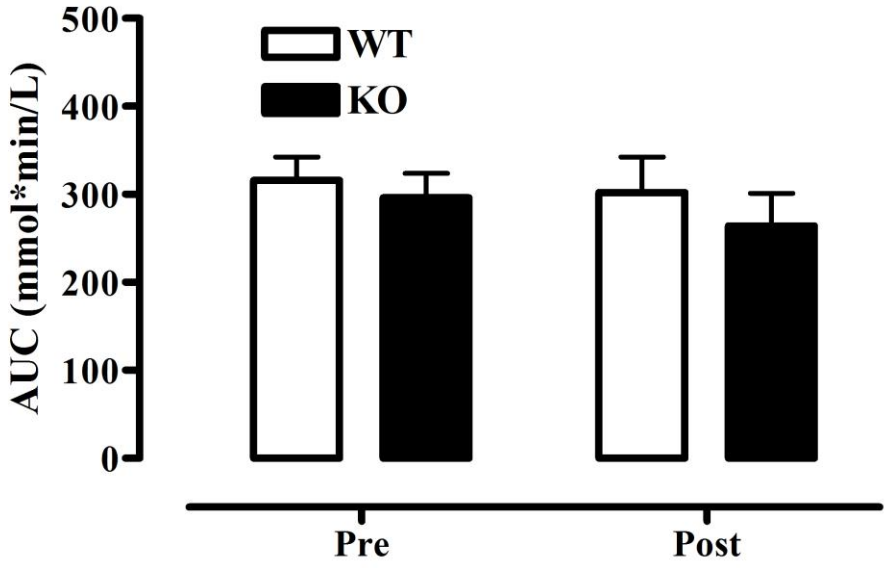

Figure 8.9. AUC for the insulin tolerance test pre- and post-HFD. (A) absolute change in plasma glucose; (B) area under the curve (AUC). There were no significant differences observed in AUC between KO and WT mice pre- or post-HFD diet ($p>0.05$). Values are means ± SE (n=13).

8.5 Western Blot Analysis

8.5.1 IRS1 Analysis

There was a main effect observed where the insulin treatment (KO and WT combined) produced a notable increase in the ratio of phosphorylated IRS1 tyr^{628} to total IRS1 protein (Fig. 8.10) compared to vehicle treated mice ($p<0.001$). Upon further analysis the standard chow fed control mice (KO and WT) exhibited a greater tyr^{628} phosphorylation of IRS1 after insulin treatment than HFD fed mice ($p<0.02$). However, there were no significant differences between KO and WT mice in total IRS1 protein expression (Fig. 8.10B) or IRS1 phospho-tyr^{628} (Fig. 8.10C) regardless of the treatment ($p>0.05$).

Analysis of ser^{307} phosphorylation of IRS1 (Fig. 8.11) revealed a main effect for diet where there was a greater phospho-ser^{307} to total IRS1 ratio in the HFD fed mice (KO and WT) compared to the standard chow fed mice ($p<0.03$). There were no differences between KO and WT mice pre- or post-HFD ($p>0.05$). All values (means ± SE) were expressed as a ratio of phospho-residue to total protein normalized to the corresponding control group.

8.5.2 Akt Analysis

Western blot analysis of Akt ser^{473} phosphorylation (Fig. 8.12C) detected no effect of insulin treatment regardless of diet ($p>0.05$). There was a non-significant trend noted where the HFD fed mice (KO and WT) exhibited a slightly greater expression of total Akt protein (Fig. 8.12B) than chow fed mice ($p=0.08$).

A small non-specific band was detected immediately below the expected Akt ser^{473} phosphorylated band (~60 kDa) on the Western blots for the anti-Akt phosho-ser^{473} antibody (Fig. 8.12A). Analysis of the unidentified band was performed due to the observation that a band was detectable in all insulin treatment mice and was absent in all non-insulin treated mice. Moreover, densitometric analysis of the non-specific band (Fig. 8.13A) revealed a significant increase in band density upon insulin stimulation in all mice (KO and WT) compared to non-insulin treated mice ($p<0.001$). Closer examination exposed a non-significant trend for a 48% and 35% decrease in the non-specific band density post-HFD in insulin treated WT and KO mice, respectively, as compared to insulin treated chow fed mice (Fig. 8.13B; $p=0.13$). There were no differences between KO and WT mice ($p>0.05$).

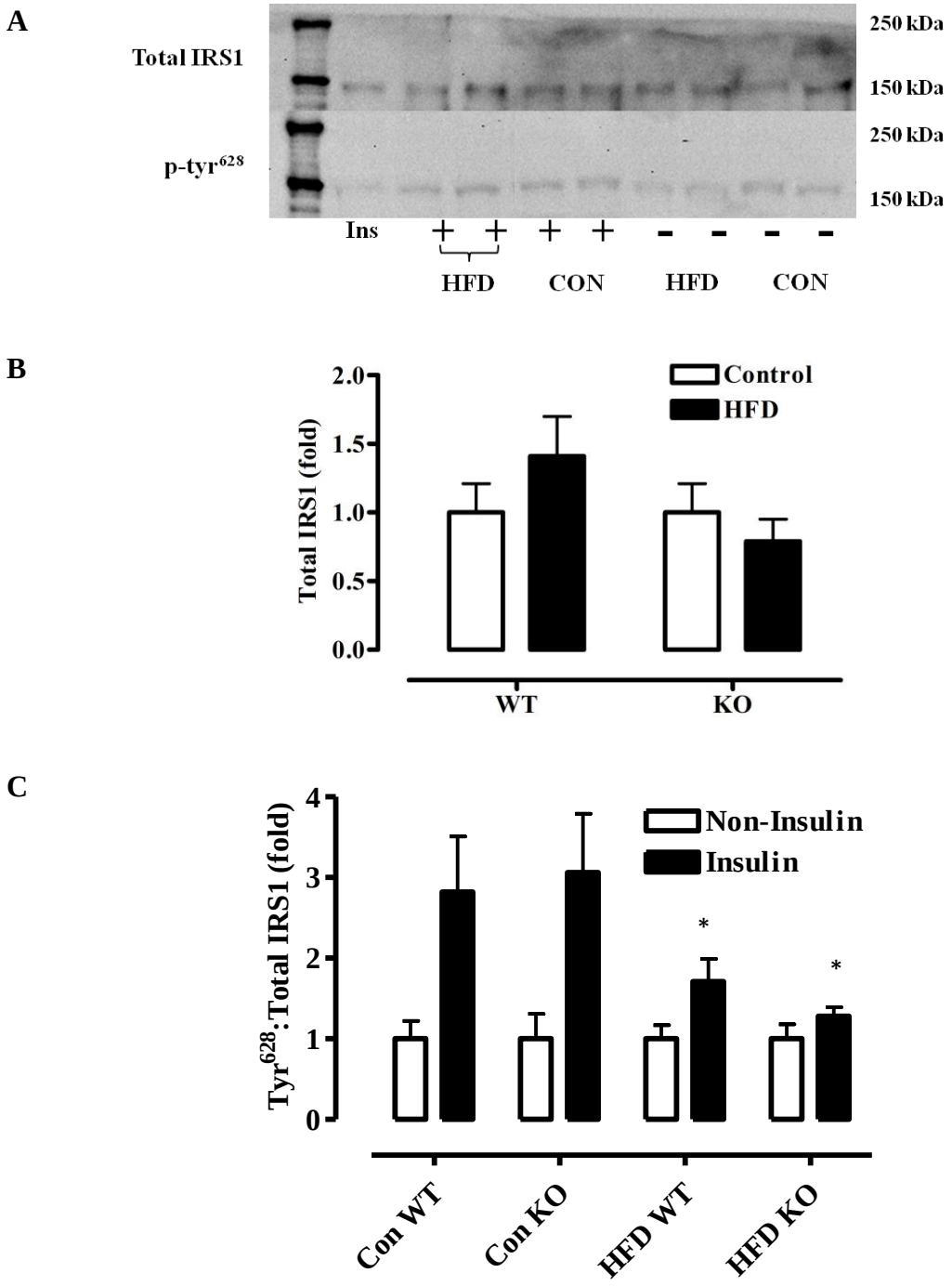

Figure 8.10: Western blot analysis of IRS1 phospho-tyr^{628} pre- and post-HFD. (A) Western blot for anti-IRS phospho-tyr^{628}; (B) total IRS1 expression; (C) phospho-tyr^{628}:total IRS. (B) There was no difference between KO and WT regardless of diet ($p>0.05$). (C) There was a main effect of insulin treatment (Ins > Non; $p<0.001$). * Significant difference compared to insulin treated Con ($p<0.02$). There was no difference between KO and WT. All values were normalized to the corresponding control group (means ± SE; tyr^{628}: n=4/4 for Con WT; n=4/6 for Con KO; n=7/8 for HFD WT; n=6/6 for HFD KO Non/Ins, respectively; total n=11 for Con WT; n=12 for Con KO; n=15 for HFD WT and KO).

A

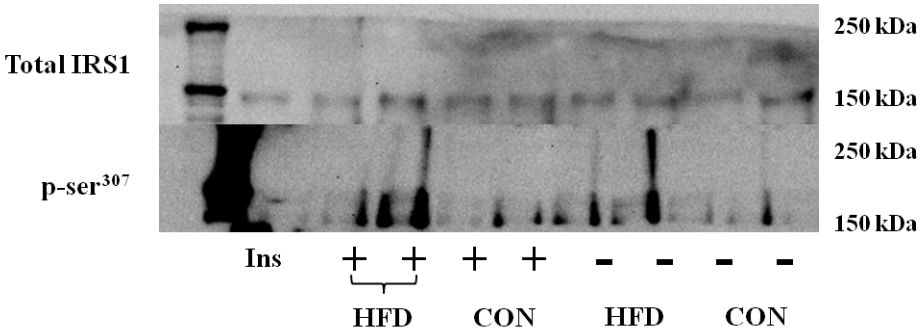

B

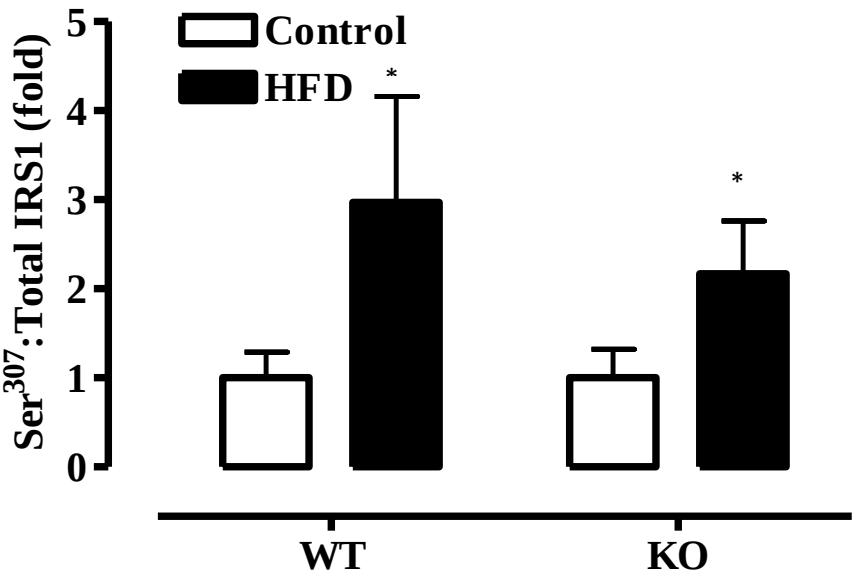

Figure 8.11. Western blot analysis of IRS1 phospho-ser^{307} pre- and post-HFD. (A) Western blot for anti-IRS phospho-ser^{307}; (B) phospho-ser^{307}:total IRS. (B) There was a main effect of diet (HFD > Con; *p<0.03;). There was no difference between KO and WT (p>0.05). All values were expressed normalized to the corresponding control group (means ± SE; ser^{307}: n=9 for Con WT; n=10 for Con KO; n=12 for HFD WT and KO).

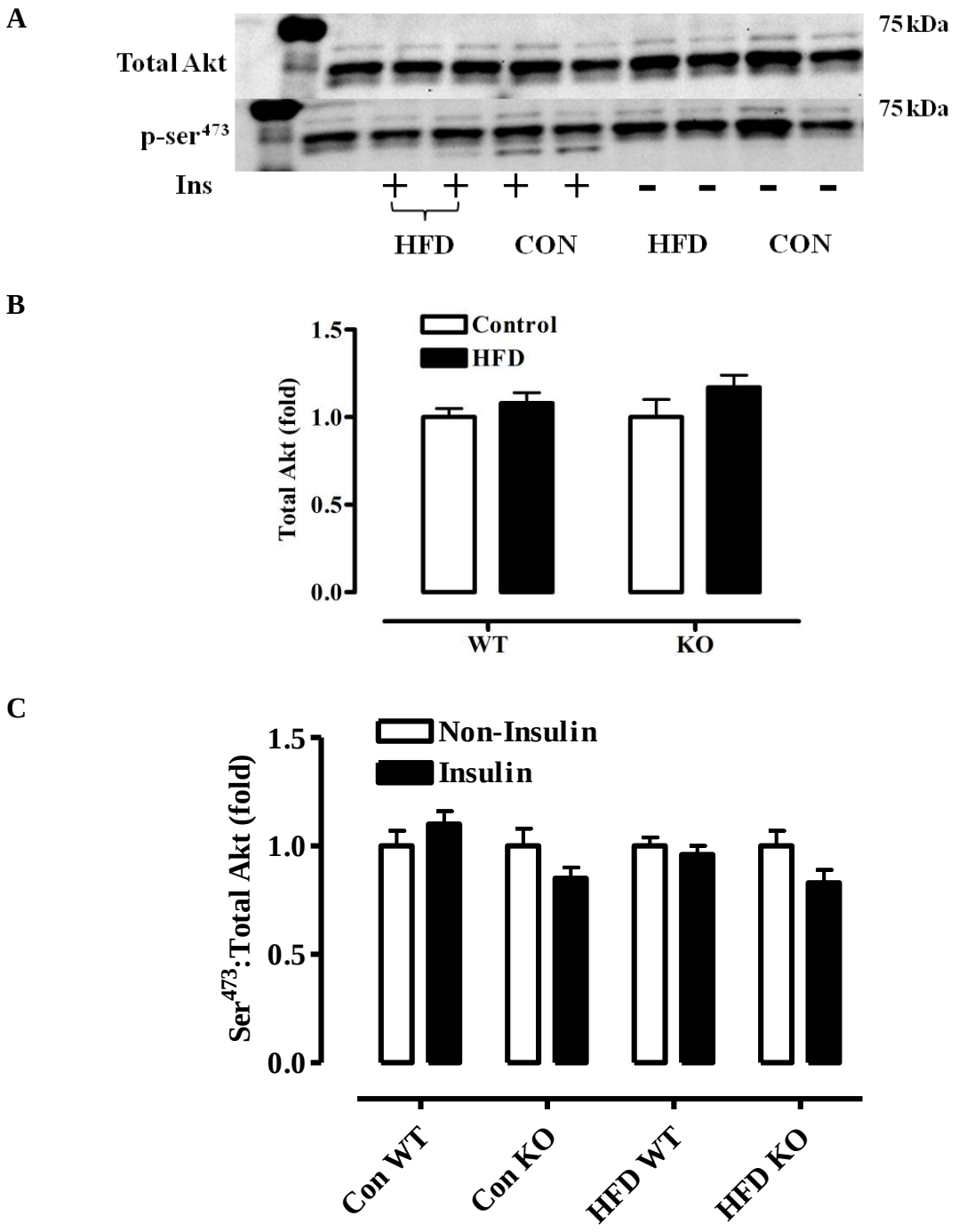

Figure 8.12. Western blot analysis of Akt phospho-ser^{473} pre- and post-HFD. (A) Western blot for anti-Akt phospho-ser^{473}; (B) total Akt protein expression; (C) phospho-ser^{473}:total Akt. (A) anti-Akt phospho-ser^{473} located at 60 kDa. There was a trend of diet where HFD fed mice exhibited a greater total Akt protein expression than chow fed mice ($p=0.08$). (C) No effect of insulin treatment (Non=Insulin) pre- or post-HFD ($p>0.05$). All values were normalized to the corresponding control group (means ± SE; n=6/5 for Con WT; n=6/6 for Con KO; n=7/8 for HFD WT and KO Non/Ins, respectively).

A

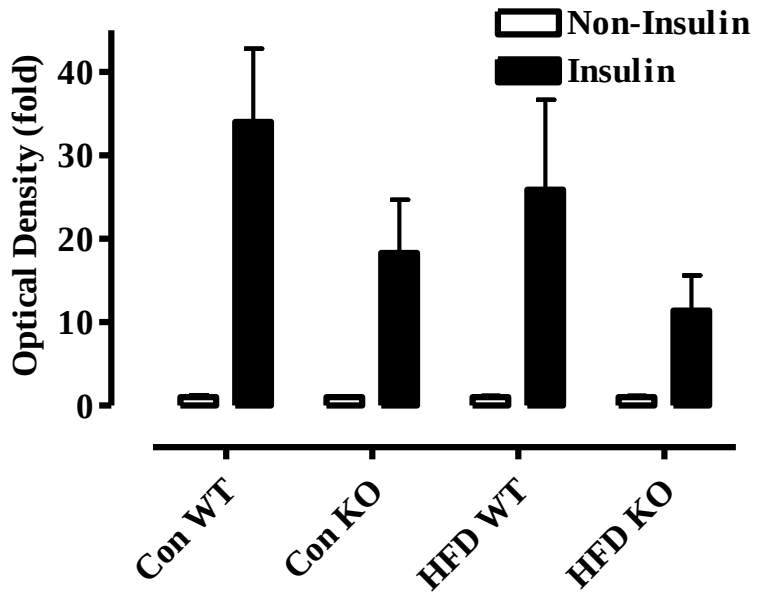

B

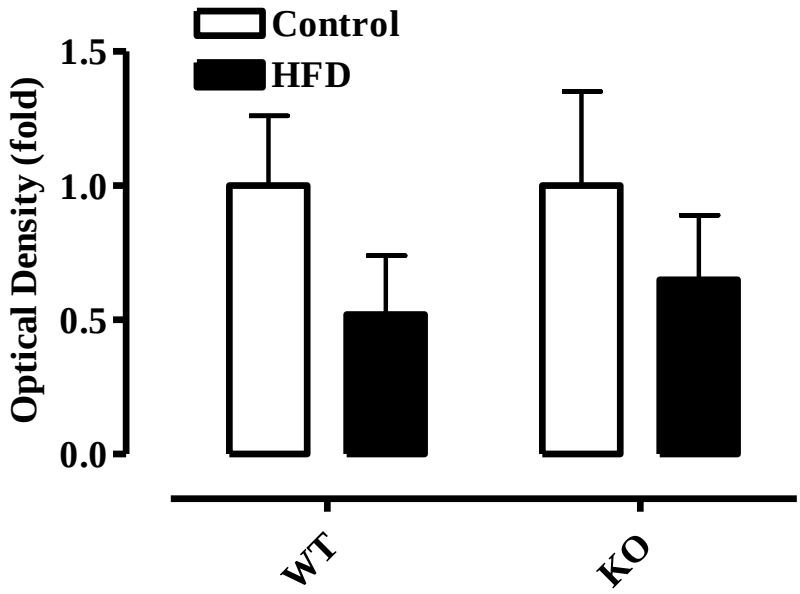

Figure 8.13. Western blot analysis of anti-Akt phospho-ser^{473} unidentified band pre- and post-HFD. (A) non-specific band of ~60 kDa; (B) insulin stimulated non-specific band pre- and post-HFD. (A) Main effect of insulin treatment (Ins>Non; $p<0.001$). (B) Main effect trend of diet (Con>HFD) following insulin stimulation ($p=0.13$). All values were normalized to the corresponding control group (means ± SE; n=6/5 for Con WT; n=6/6 for Con KO; n=7/8 for HFD WT and KO Non/Ins, respectively).

9.0 DISCUSSION

The findings of the present study confirmed previous reports that KO mice are more susceptible to obesity and its related comorbidities than wildtype mice following an 8-week high fat diet (Sayer et al., 2008; Bal et al., 2009). More specifically, the current investigation found that SLN ablation predisposes the high-fat fed mice to greater gains in whole body and retroperitoneal fat pad weight, and more severe glucose intolerance than wildtype control mice as hypothesized. In contrast to the hypothesis, there was no difference in insulin sensitivity between KO and wildtype mice following the HFD treatment.

In this study it was believed that the HFD intervention would lead to greater reductions in the phosphorylation of IRS1 tyr^{628} and Akt ser^{473}, and a larger increase in IRS1 ser^{307} phosphorylation in KO mice than control mice. Assessment of the insulin signalling cascade within skeletal muscle showed a reduction in the insulin stimulated phosphorylation of IRS1 tyr^{628} with the expected corresponding increase in IRS1 ser^{307} phosphorylation in both KO and wildtype mice after the completion of the HFD. However, there was no difference between KO and wildtype mice which is in contrast to the hypotheses. Insulin treatment did not stimulate any measurable increase in Akt ser^{473} phosphorylation in either KO or control mice regardless of the diet intervention which may reflect technical problems with the assay or a limitation with intraperitoneal insulin injections (see 9.5 Limitations). The lack of difference in IRS1 tyr^{628} phosphorylation between the genotypes suggests that the more pronounced glucose intolerance observed for the KO mice may be the result of an alternative abnormality within the glucose regulatory machinery of the KO mice.

9.1 Assessment of whole body and fat pad weight(s) following an 8-week HFD

Following the completion of the 8-week HFD the KO mice displayed a greater susceptibility to obesity as SLN ablation lead to a 20% greater increase in weight gain than high-fat fed control mice which is similar to the weight gain disparity observed in traditional rodent models of obesity such as the Otsuka Long-Evans Tokushima fatty (OLETF) rat, and the Zucker Diabetic fatty (ZDF) rat (Shima et al., 1993; Etgen & Oldham, 2000; Zhoa et al., 2008). The chronic weight gain was evident from the initial stages of the diet intervention as the KO mice gained significantly more weight at each time point starting with the first week of the diet. Upon closer examination ex vivo analysis of fat pad weights showcased the enhanced

lipogenic ability of the KO mice as the knockout mice had a larger adiposity index and fat pad weights, particularly the retroperitoneal fat pad, than wildtype mice. Interestingly, it appears that the disparity in energy balance between the genotypes is only evident in conjunction with the HFD as standard chow fed mice had no discrepancies in weight gain or adiposity. These findings raise an important issue concerning how expression of SLN can minimize the development of obesity.

Skeletal muscle has been suggested to be a principle contributor to basal metabolic rate (BMR) and therefore, total daily energy expenditure (Zurlo et al., 1990; Rolfe & Brown, 1997; Levine, 2003). There are several energy consuming processes found within muscle such as proton leak (i.e. UCP3), protein synthesis, the sodium-potassium pump, and SERCA; all of which contribute to the total energy expenditure of skeletal muscle (Rolfe & Brown, 1997). Findings from a recent study (Norris et al., 2009) suggest that the Ca^{2+} handling duties of SERCA may factor into the total energy expenditure of skeletal muscle to a greater extent than previously believed (Hasselbach & Oetliker, 1983; Clausen, Hardeveld, & Everts, 1991; Chinet et al., 1992; Dulloo, Decrouy, & Chinet, 1994). Directly inhibiting the Ca^{2+} pump with the highly specific SERCA inhibitor, cyclopiazonic acid (Goeger & Riley, 1989; Seidler et al., 1989), lead to a 50% reduction of muscle oxygen consumption in both fast- and slow-twitch isolated whole muscle preparations during resting conditions (Norris et al., 2009). During periods of elevated physical activity the proportion of energy expenditure attributed to SERCA is proposed to further increase as the magnitude of the Ca^{2+}-handling duties within the muscle cell intensifies (Zhang et al., 2006). Taken together these findings suggest an important role of SERCA in skeletal muscle energy expenditure, and thus, total daily energy expenditure.

Potentially any alteration to the efficiency of Ca^{2+} pumping by SERCA would have dramatic implications on the energy consumption of skeletal muscle. It could be assumed that the presence of SLN would influence the energy demands of Ca^{2+} pumping. In support of this notion, the co-expression of SLN and SERCA pumps in reconstituted vesicles increases the amount of heat produced in parallel to lowering the accumulation of Ca^{2+} inside the vesicles (Smith et al., 2002; Mall et al., 2006) which indicates the presence of an inefficient, futile cycle of Ca^{2+} transport. In other words, SLN uncouples ATP hydrolysis from the Ca^{2+} transport of SERCA pumps (Bombardier et al., 2008). Similarly, soleus muscle from KO mice had an approximately 10% lower contribution of SERCA towards the total oxygen consumption (i.e.

energy consumption) of skeletal muscle than wildtype mice (unpublished). The influence of the SLN:SERCA relationship towards total skeletal muscle energy expenditure appears almost insignificant considering the small overall impact that SLN:SERCA would have in relation to whole body energy expenditure. However, Butler and Kozak (2010) described a scenario where a discrepancy of approximately 5% in daily energy expenditure could result in 10-gram difference in the body weight between mice over the course of only a few months, which is in fact quite similar to the results from the present investigation. In other words, even a small disparity in energy balance can result in significant changes to body composition. Therefore, under conditions of severe energy distress, such as the exposure to a HFD, the ATP-sparing effect that SLN ablation has will predispose mice to diet-induced obesity.

9.2 Evaluation of glucose tolerance in KO mice

Standard chow fed KO mice maintained a regular glucose tolerance response to an intraperitoneal glucose load as previously described (Sayer et al., 2008). It is not until the mice are exposed to the HFD that a dramatic discrepancy in the glucose handling capabilities of the mice is observed. As expected, both the KO and wildtype mice exhibit a marked impairment in glucose tolerance following the HFD; however, the KO mice were severely more glucose intolerant than littermate controls at all time points during the 2-hour glucose tolerance test which suggests that SLN ablation has a role in glucose homeostasis. The OLETF and ob/ob rodent models of spontaneous obesity and diabetes all portray similar impairments in plasma glucose during a 2-hour glucose tolerance test as the HFD KO mice (Shima et al., 1993; Miller et al., 2008).

One possible explanation for the impaired glucose tolerance in the KO mice is that the energy imbalance and subsequent gain in adiposity, produced by the ablation of SLN, leads to an intracellular environment that obstructs the skeletal muscle GLUT4 mediated uptake of glucose from systemic circulation as described in typical cases of insulin resistance (Shulman, 2000; Morino, Petersen, & Shulman, 2006). Interestingly, KO mice display elevated plasma NEFA (unpublished). Typically, the spillover of NEFAs from adipose tissue stores into circulation results in the accumulation of intramyocellular lipid derivates, such as DAGs and ceramides, which produce the onset of insulin resistance due to the reduced activation of the insulin signalling cascade (Morino, Petersen, & Shulman, 2006; Timmers, Schrauwen, & de

Vogel, 2007; Kraegen & Cooney, 2008). There is a subsequent decrease in the translocation of GLUT4 to the cell surface which dramatically reduces glucose uptake (Shulman, 2000; Kraegen & Cooney, 2008). These findings formed the basis for examining insulin signalling in skeletal muscle in HFD KO mice in the current study.

9.3 Analysis of whole body insulin sensitivity in HFD fed KO mice

Unexpectedly, consumption of the HFD did not reduce the whole body insulin sensitivity in either KO or WT mice during the insulin tolerance test as measured by the AUC (Fig. 8.9). These results suggest that reductions in whole body insulin sensitivity may not be responsible for the observed glucose intolerance in either genotype. A common characteristic in the onset of T2DM is the continual deterioration in the ability of the peripheral tissues to adequately respond to insulin (Morino, Petersen, & Shulman, 2006; Karlsson & Zierath, 2007). Thus, it is surprising that the current study did not observe any impairment of insulin sensitivity in either HFD fed KO or WT mice. However, the insulin tolerance test is not without its limitations (Borai et al., 2007). The insulin tolerance test cannot decipher the site of the impairment in insulin action; namely, the test is unable to differentiate between hepatic or peripheral insulin resistance (Borai et al., 2007). Moreover, the increase of plasma catecholamine, glucagon, cortisol, and growth hormone levels is the classic physiological response to hypoglycaemia, all of which antagonize the insulin response and may disrupt the results of the tolerance test (Borai et al., 2007). Thus, recognizing the limitations of the insulin tolerance test it would still be plausible that skeletal muscle insulin sensitivity may be reduced in KO mice due to greater impairment of skeletal muscle insulin signalling.

9.4 Effect of the HFD on the insulin signalling pathway of KO skeletal muscle

9.4.1 Phosphorylation of IRS1 tyr^{628}

In agreement with previous reports, the standard chow fed mice (KO and WT) exhibited an approximate 3-fold increase in IRS1 tyr^{628} phosphorylation upon insulin stimulation (Griffen et al., 1999; Samuel et al., 2004; Delibegovic et al., 2007; Prada et al., 2009; Wang et al., 2009). Following the HFD there was a comparable reduction in the activation of IRS1 in both KO and wildtype mice as assessed by the amount of tyr^{628} phosphorylation. IRS1 tyr^{628} phosphorylation post-HFD was reduced to a similar extent as previously seen in ob/ob and diet-induced obese C57Bl mice (Saad et al., 1992; Hong et al., 2009; Prada et al., 2005; Prada et al., 2009).

The fact that IRS1 tyr^{628} phosphorylation is impaired after exposure to the HFD does support the notion that altered insulin signalling in skeletal muscle is contributing to the marked glucose intolerance in both KO and wildtype mice. It has been well documented that insufficient activation of IRS1 is associated with decreased PI3K recruitment, Akt phosphorylation, and GLUT4 mediated glucose uptake (Karlsson & Zierath, 2007).

9.4.2 Phosphorylation of Akt ser^{473}

The assessment of the downstream intermediate Akt did not present the expected results as insulin did not stimulate Akt ser^{473} phosphorylation in either the wildtype or KO mice pre- or post-HFD. It is possible that the timing of the insulin treatment and tissue collection was not optimal to capture the true physiological functionality of the Akt molecule. However, Morino et al. (2008) reported an 8-fold increase of Akt ser^{473} phosphorylation in chow fed wildtype C57Bl/6J mice 15-minutes post-intraperitoneal insulin injection; HFD-fed wildtype mice exhibited an approximate 60% decrease in Akt activation compared to controls (Morino et al., 2008).

The documentation associated with the anti-Akt phospho-ser^{473} antibody asserts that the phospho-ser^{473} densitometric band should be detected at approximately 60 kDa as a thick dark band. As aforementioned, analysis of this band revealed no effect of insulin on Akt ser^{473} phosphorylation (Fig. 8.12C). However, a non-specific (unidentified) insulin sensitive band was located directly below the ser^{473} band on the Western blot for anti-Akt phospho-ser^{473} (Fig. 8.12A). Densitometric analysis of the unidentified band showed a substantial increase in

phosphorylation following insulin stimulation in all mice tested pre- and post-HFD. In agreement with the literature, there was a 48% and 35% decrease in phosphorylation in HFD-fed wildtype and KO mice, respectively, compared to insulin stimulated chow fed controls (Prada et al., 2005; Zhou et al., 2007; Morino et al., 2008). Besides the noticeable trend in the data there is no evidence to suggest that the unidentified band is in fact the phospho-ser^{473} band for Akt. It is reasonable to propose that the non-specific band may be a degraded fraction of Akt, or perhaps the band is simply an unidentified alternative molecule of similar structure to Akt phosphorylated at ser^{473}. Nonetheless, it would be of interest to identify the structure of the molecule and determine whether the molecule is integral to insulin signalling in skeletal muscle.

9.4.3 Phosphorylation of IRS1 ser^{307}

The HFD initiated an approximate 2.6 fold increase in IRS1 ser^{307} phosphorylation than chow fed controls similar to previous accounts of HFD-induced ser^{307} phosphorylation (Prada et al., 2005; Adochio et al., 2009). However, there was no significant difference observed between the KO and wildtype mice. As the intramyocellular concentration of lipid metabolites (e.g. DAGs, ceramides) increases during obesity, there is a measurable increase in the activation of PKCθ which has been shown to have detrimental effects on the viability of the insulin signalling pathway (Ravichandran et al., 2000; Schmitz-Peiffer, 2000; Morino, Petersen, & Shulman, 2006). Namely, PKCθ phosphorylates several serine residues on both the insulin receptor and IRS1 substrates (near the tyrosine binding domain) (Karasik et al., 1990; Paz et al., 1997; Aguirre et al., 2002; Liu et al., 2004). The ensuing decrease in IR/IRS1 binding prohibits the expected insulin-stimulated tyrosine phosphorylation of IRS1 and activation of downstream signalling intermediates (Morino, Petersen, & Shulman, 2006). The consequence of the insulin resistance is a decrease in glucose uptake and the inability to effectively manage systemic glucose homeostasis (Morino, Petersen, & Shulman, 2006). The observed increase in IRS1 ser^{307} phosphorylation provides a plausible mechanism for the reduced phosphorylation of IRS1 tyr^{628} and related glucose intolerance in both KO and WT mice. The lack of difference in the degree of IRS1 activation post-HFD between the genotypes suggests that additional factors must negatively influence systemic glucose homeostasis in KO mice.

9.5 Proposed hypothesis for severe glucose intolerance in HFD fed KO mice

Another possibility for the severe glucose intolerance observed in the HFD fed KO mice could originate from a deficiency in insulin secretion due to a malfunction in the insulin-releasing machinery of the pancreas (Guillausseau et al., 2008). In healthy islets, β-cell depolarization initiates the rapid entry of extracellular Ca^{2+} into the β-cell which promotes the exocytosis of insulin containing vesicles to the cell surface for the release of insulin into circulation (MacDonald, Joseph, & Rorsman, 2005). Insulin release is discontinued upon cellular repolarization and Ca^{2+} uptake into the endoplasmic reticulum by SERCA2b and SERCA3 (Borge et al., 2002). Pancreatic β-cells possess a positive feedback loop where insulin acts on the β-cells to recruit IRS1 to directly interact and inhibit SERCA to prevent Ca^{2+} uptake and prolong insulin release (Borge et al., 2002). SLN, therefore, may play an intimate role in the maintenance of insulin release as SLN is a known inhibitor of SERCA Ca^{2+} transport (Odermatt et al., 1998; Asahi et al., 2002; Smith et al., 2002), and SLN mRNA has been identified in high quantities in the pancreas (European Molecular Biology Laboratory-European Bioinformatics Institute EMBL-EBI, 2010). Preliminary data on isolated β-cell islets from chow fed KO mice indicate that there is no difference in glucose-stimulated insulin secretion compared to control mice (unpublished data). This should not be surprising as the chow fed mice exhibit no measurable difference in glucose tolerance. Further investigation on islet insulin secretion from HFD fed mice is warranted as KO mice may be more susceptible to diet-induced insulin secretion deficiencies which could contribute to the onset of glucose intolerance in HFD fed KO mice.

9.6 Limitations

One of the limitations of the current investigation centers upon the use of the insulin tolerance test to assess the whole body insulin sensitivity of the mice. The insulin tolerance test is associated with several weaknesses (Borai et al., 2007); namely, the physiological response to the insulin-induced hypoglycaemia including an increase in plasma catecholamines, glucagon, cortisol, and growth hormone, all of which may interfere with the interpretation of the test (Borai et al., 2007). Moreover, the insulin tolerance test cannot differeniate between hepatic or skeletal muscle insulin resistance (Borai et al., 2007). The euglycemic-hyperinsulinemic clamp is the gold standard method for assessing insulin resistance; however, clamp studies are expensive and require specialized expertise (DeFronzo, Tobin, & Andres, 1979; Borai et al., 2007). Similarly, the concentration of the intraperitoneal injection of insulin may elicit a maximal insulin-induced glucose uptake and may mask potential differences in insulin sensitivity or activation of the insulin signalling pathway. A lower dose of insulin could expose discrepancies in the insulin sensitivity of the mice.

Several previous publications have incubated isolated muscle preparations with insulin instead of utilizing the intraperitoneal injection model (Alkhateeb et al., 2009; Mullen et al., 2009). Incubating isolated muscle preparations allows for a tighter control of insulin dosage (i.e. direct delivery to the muscle), and also avoids the confounding whole body effects of insulin and hypoglycaemia as previously mentioned (Borai et al., 2007), and thus allowing for a direct assessment of the insulin signalling pathway. However, the model employed in the current investigation does provide a representation of the whole body physiological response of glucose handling and skeletal muscle insulin signalling in the KO mice. One technique to improve the current methodology would be to collect the muscle sample during an euglycemic-hyperinsulinemic clamp, thus eliminating the insulin injection issues as well as providing information on skeletal muscle glucose disposal rate, and plasma concentrations of glucose and insulin (Adochio et al., 2009).

Another limitation of the present study was the lack of any measurable Akt ser^{473} phosphorylation upon insulin stimulation. It is possible that the timing between the insulin injection and tissue collection was not optimal for detection of Akt ser^{473} phosphorylation. The current investigation did not assess the plasma glucose concentration at the 15-minute mark during the insulin tolerance test; therefore, it is not possible to confidently conclude that

GLUT4 translocation and glucose uptake were not stimulated at this time point. Nonetheless, Morino et al. (2008) observed an approximate 8-fold increase in Akt ser^{473} phosphorylation in chow fed mice 15-minutes post insulin injection. Perhaps the assessment of insulin signalling, specifically Akt phosphorylation, in a highly oxidative skeletal muscle such as red gastrocnemius muscle instead of the whole gastrocnemius muscle collected in the present study would elicit a greater response as red oxidative muscle is more susceptible to diet-induced insulin resistance than white non-oxidative muscle (Wilkes et al., 1998). Also, red skeletal muscle exhibits a greater expression of SLN than white skeletal muscle (Babu et al., 2007b); therefore, the effect of SLN may be more evident in oxidative tissue.

One of the major limitations in the present investigation was the lack of a direct measure of GLUT4 translocation or glucose uptake. Skeletal muscle is responsible for the majority of insulin-stimulated glucose disposal (DeFronzo et al., 1981; Shulman et al., 1990), it is possible that more pronounced glucose intolerance in the HFD fed KO mice originates from an impairment in the glucose uptake capabilities of the mice.

10.0 CONCLUSION

The KO mice exhibited a greater HFD-induced increase in body and retroperitoneal fat pad weight, and displayed more pronounced glucose intolerance than HFD fed control mice. The insulin tolerance test did not reveal any measurable impairment of whole body insulin sensitivity in either KO or WT mice following the HFD. However, there was a significant reduction in the phosphorylation of IRS1 tyr^{628} in both HFD fed KO and WT mice. IRS1 ser^{307} phosphorylation was increased in both genotypes after the completion of the 8-week HFD which suggests a plausible mechanism for the reduced IRS1 tyrosine phosphorylation. In contrast to the insulin tolerance test, the Western blot data suggests that there is similar impairment in the activation of the skeletal muscle insulin signalling pathway in both genotypes. However, the results do not clarify as to why the KO mice have a dramatically reduced response during the glucose tolerance test.

The HFD fed KO mouse model exhibits similar changes in weight gain, glucose intolerance, and phosphorylation of IRS1 tyr^{628} and ser^{307} as the currently employed OLETF, ZDF, and ob/ob rodent models of diabetes (Saad et al., 1992; Shima et al., 1993; Etgen & Oldham, 2000; Prada et al., 2005; Miller et al., 2008; Zhoa et al., 2008; et al., 2009). Also, the blood profile of HFD fed KO mice (Bal et al., 2009) follows the typical disease progression for diet-induced obesity and diabetes (Alberti & Zimmet, 1998; Karlsson & Zierath, 2007). Therefore, the current investigation supports the notion that the HFD fed KO mouse is a viable and novel model of diet-induced obesity and Type II diabetes mellitus.

11.0 FUTURE DIRECTIONS

The primary goal of future investigations on the KO mouse model should focus upon further characterizing the mouse as a suitable model for T2DM. Specifically, the intramyocellular lipid profile, and the functionality of GLUT4 vesicle translocation and glucose uptake should be assessed in the KO mice following consumption of a HFD since abnormalities of these measures are classic features of diabetes (Karlsson & Zierath, 2007). Additionally, examination of pancreatic β-cell, hepatic, and adipose tissue function following the HFD intervention may provide useful insight into the greater glucose intolerance observed in the KO mice. Furthermore, the greater gain in fat mass observed for the KO mice may lead to abnormalities in the regulation of various adipokines, particularly leptin, adiponectin and TNFα, which have been associated with obesity and impairments of glucose and fat oxidation, and glucose uptake in skeletal muscle (Dyck et al., 2006).

KO mice have been shown to have a higher sub-maximal rate of oxygen consumption than wildtype mice during treadmill running (Norris et al., 2008). This disparity should also be exploited via free access to running wheels as SLN should exhibit a greater influence during periods of high SERCA activity, such as during physical activity (i.e. elevated contraction-relaxation cycling in skeletal muscle). Chronic exposure to this environment may potentially exacerbate the differences in weight gain observed between HFD fed KO and control mice, which should result in significantly greater metabolism in the wildtype mice and hence even lower susceptibility to obesity compared to KO mice.

Another avenue of interest to be examined is the overexpression of SLN in skeletal muscle and its influence on metabolic rate and diet-induced obesity. It will be important to determine the optimal level of SLN expression in skeletal muscle as overexpression may alter the functional capacity of the skeletal muscles at the cost of an elevated metabolic rate.

REFERENCES

Adams JM 2nd, Pratipanawatr T, Berria R, Wang E, DeFronzo RA, Sullards MC, & Mandarino LJ. (2004). Ceramide content is increased in skeletal muscle from obese insulin-resistant humans. Diabetes, 53(1): 25–31.

Adochio RL, Leitner W, Gray K, Draznin B, & Cornier MA. (2009). Early responses of insulin signalling to high-carbohydrate and high-fat overfeeding. Nut Metab, 6: 37-47.

Aguirre V, Werner ED, Giraud J, Lee YH, Shoelson SE, & White MF. (2002). Phosphorylation of Ser(307) in insulin receptor substrate-1 blocks interactions with the insulin receptor and inhibits insulin action. J Biol Chem, 277: 1531–1537.

Alberti KG, & Zimmet PZ. (1998). Definition, diagnosis, and classification of diabetes mellitus is complications. Diabet Med, 15: 539-553.

Alessi DR, Andjelkovic M, Caudwell B, Cron P, Morrice N, Cohen P, & Hemmings BA. (1996). Mechanism of activation of protein kinase B by insulin and IGF-1. EMBOJ, 15: 6541-6551.

Alessi DR, James SR, Downes CP, Holmes AB, Gaffney PR, Reese CB, & Cohen P. (1997). Characterization of a 3-phosphoinositide-dependent protein kinase which phosphorylates and activates protein kinase B alpha. Curr Biol, 7: 261–269.

Alkhateeb H, Chabowski A, Glatz JFC, Gurd B, Luiken JJFP, & Bonen A. (2009). Restoring AS160 phosphorylation rescues skeletal muscle insulin resistance and fatty acid oxidation while not reducing intramuscular lipids. Am J Physiol Endocrinol Metab, 297: 1056-1066.

Asahi M, Kurzydlowski K, Tada M, & MacLennan DH. (2002). Sarcolipin inhibits polymerization of phospholamban to induce superinhibition of sarco(endo)plasmic reticulum Ca2+-ATPases (SERCAs). J Biol Chem, 277: 26725-26728.

Asahi M, Sugita Y, Kurzydlowski K, De Leon S, Tada M, Toyoshima C, & MacLennan DH. (2003). Sarcolipin regulates sarco(endo)plasmic reticulum ca2+-atpase (serca) by binding to transmembrane helices alone or in association with phospholamban. PNAS, 100(9); 5040-5045.

Bai L, Wang Y, Fan J, Chen Y, Ji W, Qu A, Xu P, James DE, & Xu T. (2007). Dissecting multiple steps of GLUT4 trafficking and identifying the sites of insulin action. Cell Metab, 5: 47–57.

Babu GJ, Bhupathy P, Timofeyev V, Petrashevskaya NN, Reiser P J, Chiamvimonvat N, & Periasamy M. (2007a). Ablation of sarcolipin enhances sarcoplasmic reticulum calcium transport and atrial contractility. PNAS, 104: 17867-17872.

Babu GJ, Bhupathy P, Carnes CA, Billman GE, & Periasamy M. (2007b). Differential expression of sarcolipin protein during muscle development and cardiac pathophysiology. J Mol Cell Cardiol, 42: 215-222.

Bal NC, Gupta SC, Bombardier E, Sayer RA, Norris SM, Tupling AR, & Periasamy M. (2009). Sarcolipin is a novel regulator of metabolism and obesity. Obesity, 17(S2): S49-S50.

Bandyopadhyay GK, Yu JG, Ofrecio J, & Olefsky JM. (2006). Increased malonyl-CoA levels in muscle from obese and type 2 diabetic subjects lead to decreased fatty acid oxidation and increased lipogenesis; thiazolidinedione treatment reverses these defects. Diabetes, 55: 2277–2285.

Baribault H. (2010). Mouse models of type II diabetes mellitus in drug discovery. New York: Humana Press.

Blaxter K. (1989). Energy metabolism in animals and man. Cambridge: Cambridge University Press.

Befroy DE, Petersen KF, Dufour S, Mason GF, de Graaf RA, Rothman DL, & Shulman GI. (2007). Impaired mitochondrial substrate oxidation in muscle of insuin-resistant offspring of type 2 diabetic patients. Diabetes, 56: 1376-1381.

Bergman RN, Prager R, Volund A, & Olefsky JM. (1987). Equivalence of insulin sensitivity index in man derived by the minimal model method and the euglycemic glucose clamp. J Clin Invest, 79: 790-800.

Bergman RN. (1989). Toward physiological understanding of glucose tolerance: minimal-model approach. Diabetes, 38: 1512-1527.

Blakemore AI, & Froguel P. (2008). Is obesity our genetic legacy?. J Clin Endocrinol Metab, 93: S51-S56.

Bloomgarden ZT. (2000). American Diabetes Association Annual Meeting, 1999: diabetes and obesity. Diabetes Care 23: 118–124.

Boden G, Jadali F, White J, Liang Y, Mozzoli M, Chen X, Coleman E, & Smith C. (1991). Effects of fat on insulin-stimulated carbohydrate metabolism in normal men. J Clin Invest, 88: 960-966.

Boden G, Chen X, DeSantis RA, & Kendrick Z. (1993). Effects of age and body fat on insulin resistance in healthy men. Diabetes Care, 16: 728-733.

Boden G, & Chen X. (1995). Effects of fat on glucose uptake and utilization in patients with non-insulin-dependent diabetes. J Clin Invest, 96: 1261-1268.

Boden G. (1997). Role of fatty acids in the pathogenesis of insulin resistance and NIDDM. Diabetes, 46: 3-10.

Boden G. (2001). Pathogenesis of type 2 diabetes. Endo Metab Clin NA, 30(4): 801-815.

Boden G, Lebed B, Schatz M, Homko C, & Lemieux S. (2001). Effects of acute changes of plasma free fatty acids on intramyocellular fat content and insulin resistance in healthy subjects. Diabetes, 50: 1612-1617.

Bombardier E, Vigna C, Babu G, Backx PH, Periasamy M, MacLennan DH, Gramolini AO, & Tupling AR. (2008). SLN ablation increases Ca2+ pump efficiency in skeletal muscle. FASEB J, 22: 1157.5.

Bonen A, Parolin ML, Steinberg GR, Calles-Escandon J, Tandon NN, Glatz JFC, Luiken JJFP, Heigenhauser GJF, & Dyck DJ. (2004). Triacylglycerol accumulation in human obesity and type 2 diabetes is associated with increased rates of skeletal muscle fatty acid transport and increased sarcolemmal FAT/CD36. FASEB J, 18: 1144–1146.

Bonnard C, Durand A, Peyrol S, Chanseaume E, Chauvin MA, Morio B, Vidal H, & Rieusset J. (2008). Mitochondrial dysfunction results from oxidative stress in the skeletal muscle of diet-induced insulin-resistant mice. J Clin Invest, 118: 789-800.

Borai A, Livingstone C, & Ferns GA. (2007). The biochemical assessment of insulin resistance. Ann Clin Biochem, 44: 324-342.

Borge PD, Moibi J, Greene SR, Trucco M, Young RA, Gao Z, & Wolf BA. (2002). Insulin receptor signalling and sarco/endoplasmic reticulum calcium ATPase in β-cells. Diabetes, 51(S3): S427-S433.

Bornemann A, Ploug T, & Schmalbruch H. (1992). Subcellular localization of GLUT4 in nonstimulated and insulin-stimulated soleus muscle of rat. Diabetes, 41: 215–221.

Bruss MD, Arias EB, Lienhard GE, & Cartee GD. (2005). Increased phosphorylation of Akt substrate of 160 kDa (AS160) in rat skeletal muscle in response to insulin or contractile activity. Diabetes, 54(1): 41-50.

Butler AA, & Kozak LP. (2010). A recurring problem with the analysis of energy expenditure in genetic models expressing lean and obese phenotypes. Diabetes, 59: 323-329.

Canadian Diabetes Association (CDA). (2008) Clinical practice guidelines for the prevention and management of diabetes in Canada. Can J Diabetes, 32(S1): S1-S201.

Canadian Diabetes Association (CDA). (2009). The prevalence and costs of diabetes. Retrieved from: http://www.diabetes.ca/documents/about-diabetes/PrevalanceandCost_09.pdf

Carley AN, & Severson DL. (2005). Fatty acid metabolism is enhanced in type 2 diabetic hearts. Biochim Biophys Acta, 1734: 112–126.

Carley AN, Atkinson LA, Bonen A, Harper ME, Kunnathu S, Lopaschuk GD, & Severson DL. (2007). Mechanisms responsible for enhanced fatty acid utilization by perfused hearts from type 2 db/db mice. Arch Physiol Biochem, 113: 65–75.

Cartee GD, & Wojtaszewski JFP. (2007). Role of Akt substrate 160 kDa in insulin-stimulated and contraction-stimulated glucose transport. Appl Physiol Nutr Metab, 32: 557-566.

Chabowski A, Chatham JC, Tandon NN, Calles-Escandon J, Glatz JFC, Luiken JJFP, & Bonen A. (2006). Fatty acid transport and FAT/CD36 are increased in red but not in white muscle skeletal muscle of Zucker diabetic fatty (ZDF) rats. Am J Physiol Endocrinol Metab, 291: E675–E682.

Chalkley SM, Hettiarachchi N, Chisholm DJ, & Kraegen EW. (1998). Five-hour fatty acid elevation increases muscle lipids and impairs glycogen synthesis in the rat. Metabolism, 47: 1121–1126.

Charron MJ, Brosius FC III, Alper SL, & Lodish HF. (1989). A glucose transport protein expressed predominately in insulin-responsive tissues. PNAS, 86: 2535–2539.

Chavez JA, Knotts TA,Wang LP, Li G, Dobrowsky RT, Florant GL, Summers SA. (2003). A role for ceramide, but not diacylglycerol, in the antagonism of insulin signal transduction by saturated fatty acids. J Biol Chem, 278: 10297–10303.

Chen D, & Wang MW. (2005). Development and application of rodent models for type 2 diabetes. Diab, Obes, & Metab, 7: 307-317.

Chibalin AV, Leug Y, Vieira E, Krook A, Björnholm M, Long YC, Kotova O, Zhong Z, Sakane F, Steiler T, Nylén C, Wang J, Laakso M, Topham MK, Gilbert M, Wallberg-Henriksson H, & Zierath JR. (2008). Downregulation of diacylglycerol kinase delta contributes to hyperglycemia-induced insulin resistance. Cell, 132: 375-386.

Cho H, Mu J, Kim JK, Thorvaldsen JL, Chu Q, Crenshaw EB, Kawstner KH, Bartolomei MS, Shulman GI, & Birnbaum MJ. (2001a). Insulin resistance and a diabetes mellitus-like syndrome in mie lacking the protein kinase Akt2 (PKBbeta). Science, 292: 1728-1731.

Cho H, Thorvaldsen JL, Chu Q, Feng F, & Birnbaum MJ. (2001b). Akt1/PKBalpha is required for normal growth but dispensable for maintenance of glucose homeostasis in mice. J Biol Chem, 276: 38349-38352.

Clausen T, Van Hardeveld C, & Everts ME. (1991). Significance of cation transport in control of energy metabolism and thermogenesis. Physiol Rev, 71: 733-774.

Cline GW, Petersen KF, Krssak M, Shen J, Hundal RS, Trajanoski Z, Inzucchi S, Dresner A, Rothman DL, Shulman GI. (1999). Impaired glucose transport as a cause of decreased

insulin-stimulated muscle glycogen synthesis in type 2 diabetes. N Engl J Med 341:240 –246.

Cline GW, Johnson K, Regittnig W, Perret P, Tozzo E, Xiao L, Damico C, & Shulman GI. (2002). Effects of a novel glycogen synthase kinase-3 inhibitor on insulin-stimulated glucose metabolism in Zucker diabetic fatty (fa/fa) rats. Diabetes 51: 2903–2910.

Chinet A, Decrouy A, & Even PC. (1992). Ca2+-dependent heat production under basal and near-basal conditions in the mouse soleus muscle. J Physiol, 455: 663-678.

Coleman DL. (1980). Lessons from studies with genetic forms of diabetes in the mouse. Metab, 32: 162-164.

Coleman DL. (1982). Obese and diabetes: two mutant genes causing diabetes-obesity syndromes in mice. Diabetes, 31(S1): 1-6.

Coort SLM, Hasselbaink DM, Koonen DPY, Willems J, Coumans WA, Chabowski A, van der Vusse GJ, Bonen A, Glatz JFC, & Luiken JJFP. (2004a). Enhanced sarcolemmal FAT/CD36 content and triacylglycerol storage in cardiac myocytes from obese Zucker rats. Diabetes 53: 1655–1663.

Coort SLM, Luiken JJFP, van Der Vusse GJ, Bonen A, & Glatz JFC. (2004b). Increased FAT (fatty acid translocase)/CD36-mediated longchain fatty acid uptake in cardiac myocytes from obese Zucker rats. Biochem Soc Trans 32: 83–85.

Cushman SW, & Wardzala LJ. (1980). Potential mechanism of insulin action on glucose transport in the isolated rat adipose cell: apparent translocation of intracellular transport systems to the plasma membrane. J Biol Chem, 255: 4758–4762.

Damsbo P, Vaag A, Hother-Nielsen O, & Beck-Nielsen H. (1991). Reduced glycogen synthase activity in skeletal muscle from obese patients with and without type 2 (non-insulin-dependent) diabetes mellitus. Diabetologia, 34: 239-245.

DeFronzo RA, Tobin JD, & Andres R. (1979). Glucose clamp technique: a method for quantifying insulin secretion and resistance. Am J Physiol, 237: E214-E223.

DeFronzo RA, Jocot E, Jequier E, Maeder E, Wahren J, & Felber JP. (1981). The effect of insulin on the disposal of intravenous glucose. Results from indirect calorimetry and hepatic and femoral venous catheterization. Diabetes, 30: 1000-1007.

Delibegovic M, Bence KK, Mody N, Hong EG, Ko HJ, Kim JK, Kahn BB, & Neel BG. (2007). Improved glucose homeostasis in mice with muscle-specific deletion of protein-tyrosine phosphatise 1b. Molec Cell Biol, 27(21): 7727-7734.

Deurenberg P, Andreoli A, Borg P, Kukkonen-Harjula K, de Lorenzo A, van Marken Lichtenbelt WD, Testolin G, Vigano R, & Vollaard N. (2001). The validity of predicted

body fat percentage from body mass index and from impedance in samples from five European populations. Euro J Clin Nutr, 55: 973-979.

Diabetes Prevention Program Research Group (DPPRG). (2005). Role of insulin secretion and sensitivity in the evolution of type 2 diabetes in the diabetes prevention program: effects of lifestyle intervention and metformin. Diabetes, 54: 2404 –2414.

Dobbins RL, Szczepaniak LS, Bentley B, Esser V, Myhill J, & McGarry JD. (2001). Prolonged inhibition of muscle carnitine palmitoyltransferase-1 promotes intramyocellular lipid accumulation and insulin resistance in rats. Diabetes, 50: 123–130.

Dobrowsky RT, Kamibayashi C, Mumby MC, & Hannun YA. (1993). Ceramide activates heterotrimeric protein phosphatise 2A. J Biol Chem, 268: 15523–15530.

Donnelly R, Reed MJ, Azhar S, & Reaven GM. (1994). Expression of the major isoenzyme of protein kinase-C in skeletal muscle, nPKC theta, varies with muscle type and in response to fructose-induced insulin resistance. Endocrinology, 135: 2369–2374.

Dresner A, Laurent D, Marcucci M, Griffen ME, Dufour S, Cline GW, Slezak LA, Andersen DK, Hundal RS, Rothman DL, Petersen KL, & Shulman GI. (1999). Effects of free fatty acids on glucose transport and IRS-1-associated phophatidylinositol 3-kinase activity. J Clin Invest, 103: 253-259.

Dubuc PU. (1976). The development of obesity, hyperinsulinemia, and hyperglycemia in ob/ob mice. Metabolism, 25(12): 1567-1574.

Dulloo AG, Decrouy A, & Chinet A. (1994). Suppression of Ca2+-dependent heat production in mouse skeletal muscle by high fish oil consumption. Metabolism, 43: 931-934.

Dyck DJ, Heigenhauser GJ, & Bruce CR. (2006). The role of adipokines as regulator of skeletal muscle fatty acid metabolism and insulin sensitivity. Acta Physiol, 186: 5-16.

Ellis BA, Poynten A, Lowy AJ, Furler SM, Chisholm DJ, Kraegen EW, & Cooney GJ. (2000). Long-chain acyl-CoA esters as indicators of lipid metabolism and insulin sensitivity in rat and human muscle. Am J Physiol Endocrinol Metab, 279: E554–E560.

Etgen GH, & Oldham BA. (2000). Profiling of Zucker diabetic fatty rats in their progression to the overt diabetic state. Metabolism, 49: 684-688.

Ferrannini E, Natali A, Bell P, et al. (1997). Insulin resistance and hypersecretion in obesity. J Clin Invest, 100: 1166-1173.

Flegal KM, Graubard BI, Williamson DF, & Gail MH. (2007). Cause-specific excess deaths associated with underweight, overweight, and obesity. JAMA, 298: 2028–2037.

Fueger PT, Bracy DP, Malabanan CM, Pencek RR, Granner DK, & Wasserman DH. (2004). Hexokinase II overexpression improves exercise-stimulated but not insulin-stimulated muscle glucose uptake in high-fat-fed C57BL/6J mice. Diabetes 53:306 –314.

Fujii N, Boppart MD, Dufresne SD, Crowley PF, Jozsi AC, Sakamoto K, Yu H, Aschenbach WG, Kim S, Miyazaki H, Rui L, White MF, Hirschman MF, & Goodyear LJ. (2004). Overexpression or ablation of JNK in skeletal muscle has no effect on glycogen synthase activity. Am J Physiol Cell Physiol, 287: C200-C208.

Fukomoto H, Kayano T, Buse JB, Edwards Y, Pilch PF, Bell GI, & Seino S. (1989). Cloning and characterization of the major insulin-responsive glucose transporter expressed in human skeletal muscle and other insulin-responsive tissues. J Biol Chem, 264(14): 7776-7779.

Glatz JF, Luiken JF, & Bonen A. (2010). Membrane fatty acid transporters as regulators of lipid metabolism: implications for metabolic disease. Physiol Rev, 90: 367-417.

Goeger DE, & Riley RT. (1989). Interaction of cyclopiazonic acid with rat skeletal muscle sarcoplasmic reticulum vesicles. Biochem Pharmacol, 38: 3995-4003.

Goodpaster BH, He J, Watkins S, & Kelley DE. (2001). Skeletal muscle lipid content and insulin resistance: evidence for a paradox in endurance trained athletes. J Clin Endocrinol Metab, 86: 5755–5761.

Gonzalez E, & McGraw TE. (2006). Insulin signalling diverges into Akt dependent and independent signals to regulate recruitment/docking and the fusion GLUT4 vesicles to the plasma membrane. Mol Biol Chem, 17: 4484-4493.

Gorden ES. (1960). Non-esterified fatty acids in blood of obese and lean subjects. Am J Clin Nutr, 8: 740.

Griffen ME, Marcucci MJ, Cline GW, Bell K, Barucci N, Lee D, Goodyear LJ, Kraegen EW, White MF, & Shulman GI. (1999). Free fatty acid-induced insulin resistance is associated with activation of protein kinase C theta and alterations in the insulin signaling cascade. Diabetes, 48: 1270–1274.

Guillausseau PJ, Meas T, Virally M, Laloi-Michelin M, Médeau V, & Kevorkian JP. (2008). Abnormalities in insulin secretion in type 2 diabetes mellitus. Diab Metab, 34(S2): S43-S48.

Han XX, Chabowski A, Tandon NN, Calles-Escandon J, Glatz JF, Luiken JJ, & Bonen A. (2007). Metabolic challenges reveal impaired fatty acid metabolism and translocation of FAT/CD36 but not FABPpm in obese Zucker rat muscle. Am J Physiol Endocrinol Metab 293: E566–E575.

Hancock CR, Han DH, Chen M, Terada S, Yasuda T, Wright DC, & Holloszy JO. (2008). High-fat diets cause insulin resistance despite an increase in muscle mitochondria. PNAS, 105(22): 7815-7820.

Hasselbach W, & Oetliker H. (1983). Energetics and electrogenicity of the sarcoplamic reticulum calcium pump. Ann Rev Physiol, 45: 325-339.

Hegarty BD, Cooney GJ, Kraegen EW, & Furler SM. (2002). Increased efficiency of fatty acid uptake contributes to lipid accumulation in skeletal muscle of high fat-fed insulin-resistant rats. Diabetes, 51: 1477–1484.

Hirosumi J, Tuncman G, Chang L, Görgün CZ, Uysal KT, Maeda K, Karin M, & Hotamisligil GS. (2002). A central role for JNK in obesity and insulin resistance. Nature, 420(6913): 333-336.

Holland WL, Knotts TA, Chavez JA, Wang LP, Hoehn KL, & Summers SA. (2007a). Lipid mediators of insulin resistance. Nutr Rev, 65: S39-S46.

Holland WL, Brozinick JT, Wang LP, Hawkins ED, Sargent KM, Liu Y, Narra K, Hoehn KL, Knotts TA, Siesky A, Nelson DH, Karathanasis SK, Fontenot GK, Birnbaum MJ, & Summers SA . (2007b). Inhibition of ceramide synthesis ameliorates glucocorticoid-, saturated fat-, and obesity-induced insulin resistance. Cell Metab, 5: 167-179.

Holloway GP, Benton CR, Mullen KL, Yoshida Y, Snook LA, Han XX, Glatz JFC, Luiken JJFP, Lally J, Dyck DJ, & Bonen A. (2009). In obese rat muscle transport of palmitate is increased and is channeled to triacylglycerol storage despite an increase in mitochondrial palmitate oxidation. Am J Physiol Endocrinol Metab, 296: E738–E747.

Hong EG, Ko HJ, Cho YR, Kim HJ, Ma Z, Yu TY, Friedline RH, Kurt-Jones E, Finberg R, Fischer MA, Granger EL, Norbury CC, Hauschka SD, Philbrick WM, Lee CG, Elias JA, & Kim JK. (2009). Interleukin-10 prevents diet-induced insulin resistance by attenuating macrophage and cytokine response in skeletal muscle. Diabetes, 58(11): 2525-2535.

Huang C, Thirone ACP, Huang X, & Klip A. (2005). Differential contribution of insulin receptor substrates 1 versus 2 to insulin signalling and glucose uptake in L6 myotubes. J Biol Chem, 280: 19426-35.

International Diabetes Federation (IDF). (2007). United for diabetes campaign: key messages. Belgium, retrieved from: http://www.unitefordiabetes.org/assets/files/UNR_key_messages_20060828.pdf.

Ishikura S, Bilan PJ, & Klip A. (2007). Rabs 8A and 14 are targets of the insulin-regulated Rab-GTP AS160 regulating GLUT4 traffic in muscle cell. Biochem Biophys Res Commun, 353(4): 1074-1079.

Itani SI, Pories WJ, MacDonald KG, & Dohm GL. (2001). Increased protein kinase C theta in skeletal muscle of diabetic patients. Metab, 50: 553–557.

Itani SI, Ruderman NB, Schmieder F, & Boden G. (2002). Lipid-induced insulin resistance in human muscle is associated with changes in diacylglycerol, protein kinase C, and I kappa B-alpha. Diabetes 51: 2005–2011.

James DE, Strube M, & Mueckler M. (1989). Molecular cloning and characterization of an insulin-regulatable glucose transporter. Nature, 338: 83–87.

Jensen TE, Rose AJ, Hellsten Y, Wojtaszewski JF, & Richter ER. (2007). Caffeine-induced Ca(2+) release increases AMPK-dependent glucose uptake in rodent soleus muscle. Am J Physiol Endocrinol Metab, 293(1): E286-E292.

Kaburagi Y, Satoh S, Tamemoto H, Yamamoto-Honda R, Tobe K, Veki K, Yamauchi T, Kono-Sugita E, Sekihara H, Aizawa S, Cushman SW, Akanuma Y, Yazaki Y, & Kadowaki T. (1997). Role of insulin receptor substrate-1 and pp60 in the regulation of insulin-induced glucose transport and GLUT4 translocation in primary adipocytes. J Biol Chem, 272(41): 25839-44.

Karasik A, Rothenberg PL, Yamada K, White MF, & Kahn CR. (1990). Increased protein kinase C activity is linked to reduced insulin receptor autophosphorylation in liver of starved rats. J Biol Chem, 265: 10226–31.

Karlsson HK, Zierath JR, Kane S, Krook A, Lienhard GE, & Wallberg-Henriksson H. (2005). Insulin-stimulated phosphorylation of the Akt substrate AS160 is impaired in skeletal muscle of type 2 diabetic subjects. Diab, 54(6): 1692-7.

Karlsson HKR, & Zierath JR. (2007). Insulin signalling and glucose transport in insulin resistant human skeletal muscle. Cell Biochem Biophys, 48: 103-113.

Katzmarzyk PT, & Janssen I. (2004). The economic costs associated with physical inactivity and obesity in Canada: an update. Can J Appl Physiol, 29: 90–115.

Katzmarzyk PT, & Mason C. (2006). Prevalence of class I, II, and III obesity in Canada. Can Med Assoc J, 174(2): 156-157.

Kawano K, Hirashima T, Mori S, Saitoh Y, Kurosumi M, & Natori T. (1992). Spontaneous long-term hyperglycaemic rat with diabetic complications. Otsuka Long-Evans Tokushima Fatty (OLETF) Strain. Diabetes, 41: 1422-1428.

Kawano K, Hirashima T, Mori S, & Natori T. (1994). OLETF (Otsuka Long-Evans Tokushima Fatty) rat: a new NIDDM rat strain. Diabetes Res Clin Pract, 24(Suppl.): S317-S320.

Kido Y, Burks DJ, Withers D, Bruning JC, Kahn CR, White MF, & Accili D. (2000). Tissue-specific insulin resistance in mice with mutations in the insulin receptor, irs-1, and irs-2. J Clin Invest, 105: 199-205.

Kiens B. (2006). Skeletal muscle lipid metabolism in exercise and insulin resistance. Physiol Rev, 86: 205-243.

Kim JK, Fillmore JJ, Sunshine MJ, Albrecht B, Higashimori T, Kim DW, Liu ZX, Soos TJ, Cline GW, O'Brien WR, Littman DR, & Shulman GI. (2004). PKC-theta knockout mice are protected from fat-induced insulin resistance. J Clin Invest 114:823– 827.

Kopelman P. (2007). Health risks associated with overweight and obesity. Obes Rev, 8(S1): 13-17.

Kraegen EW, Clark PW, Jenkins AB, Daley EA, Chrisholm DJ, & Storlien H. (1991). Development of muscle insulin resistance after liver insulin resistance in high-fat fed rats. Diabetes, 40: 1397-1403.

Kraegen EW & Cooney GJ. (2008). Free fatty acids and skeletal muscle insulin resistance. Curr Opin Lipid, 19: 235-241.

Kraegen EW, Cooney GJ, Turner N. (2008). Muscle insulin resistance: a case of fat overconsumption, not mitochondrial dysfunction. PNAS, 105(22): 7627-7628.

Krook A, Wallberg-Henriksson H, & Zierath JR. (2004). Sending the signal: molecular mechanisms regulating glucose uptake. Med Sci Sport Exer. 36(7): 1212-7.

Laemmli UK. (1970). Cleavage of structural proteins during the assembly of the head of bacteriophage T4. Nature, 227: 680-685.

Lara-Castro C, Newcomer BR, Rowell J, Wallace P, Shaughnessy SM, Munoz AJ, Shiflett AM, Rigsby DY, Lawrence JC, Bohning DE, Buchtal S, & Garvey WT. (2008). Effects of short-term very low-calorie diet on intramyocellular lipid and insulin sensitivity in nondiabetic and type 2 diabetic subjects. Metab Clin Exp, 57: 1-8.

Larance M, Ramm G, Stockli J, van Dam EM, Winata S, Wasinger V, Simpson F, Graham M, Junutula JR, Guilhaus M, & James DE. (2005). Characterization of the role of the Rab GTPase-activating protein AS160 in insulin-regulated GLUT4 trafficking. J Biol Chem, 280: 37803–37813.

Leney SE, & Tavare JM. (2009). The molecular basis of insulin-stimulated glucose uptake: signalling, trafficking and potential drug targets. J Endocrin, 203: 1-18.

Levine JA. (2003). Non-exercise activity thermogenesis. Proc Nutr Soc, 62: 667-679.

Levy J, Gavin JR, & Sowers JR. (1994). Diabetes mellitus: a disease of abnormal cellular calcium metabolism. Am J Med, 96(3): 260-273.

Li B, Nolte LA, Ju JS, Han DH, Coleman T, Holloszy JO, Semenkovich CF. (2000). Skeletal muscle respiratory uncoupling prevents diet-induced obesity and insulin resistance in mice. Nature Med, 6(10): 1115-1120.

Lillioja S, Mott DM, Spraul M, Ferraro R, Foley JE, Ravussin E, Knowler WC, Bennett PH, & Bogardus C. (1993). Insulin resistance and insulin secretory dysfunction as precursors of non-insulin-dependent diabetes mellitus: prospective studies of Pima Indians. N Engl J Med, 329: 1988 –1992.

Lipscombe LL, & Hux JE. (2007). Trends in diabetes prevalence, incidence, and mortality in Ontario, Canada 1995-2005: a population based study. The Lancet, 369(9563): 750-756.

Liu YF, Herschkovitz A, Boura-Halfon S, Ronen D, Paz K, Leroith D, & Zick Y. (2004). Serine phosphorylation proximal to its phosphotyrosine binding domain inhibits insulin receptor substrate 1 function and promotes insulin resistance. Mol Cell Biol, 24: 9668–9681.

Liu L, Zhang Y, Chen N, Shi X, Tsang B, & Yu YH. (2007). Upregulation of myocellular DGAT1 augments triglyceride synthesis in skeletal muscle and protects against fat-induced insulin resistance. J Clin Invest, 117: 1679-1689.

Luiken JJFP, Arumugam Y, Dyck DJ, Bell RC, Pelsers ML, Turcotte LP, Tandon NN, Glatz JFC, & Bonen A. (2001). Increased rates of fatty acid uptake and plasmalemmal fatty acid transporters in obese Zucker rats. J Biol Chem, 276: 40567–40573.

MacDonald PE, Joseph JW, & Rorsman P. (2005). Glucose-sensing mechanisms in pancreatic β-cells. Phil Trans R Soc B, 360: 2211-2225.

Mall S, Broadbridge R, Harrison SL, Gore MG, Lee AG, & East JM. (2006). The presence of sarcolipin results in increased heat production by Ca^{2+}-ATPase. J Biol Chem, 281(48): 36597-36602.

Mattsson S, & Thomas BJ. (2006). Development of methods for body composition studies. Phys Med Biol, 51: R203-R228.

Merrill Jr AH. (2002). De novo sphingolipid biosynthesis: a necessary, but dangerous, pathway. J Biol Chem, 277: 25843–25846.

Merrill RM, & Richardson JS. (2009). Validity of self-reported height, weight, and body mass index: findings from the National Health and Nutrition Examination survey, 2001-2006. Prev Chronic Dis, 6(4): A121.

Mîinea CP, Sano H, Kane S, Sano E, Fukuda M, Peränen J, Lane WS, & Lienhard GE. (2005). AS160, the Skt substrate regulating GLUT4 translocation, has a functional Rab GTPase-activing protein domain. Biochem J, 391: 87-93.

Miller AM, Brestoff JR, Phelps CB, Berk EZ, & Reynolds TH. (2008). Rapamycin does not improve insulin sensitivity despite elevated mammalian target of rapamycin complex 1 activity in muscles of ob/ob mice. Am J Physiol Regul Integr Comp Physiol, 295(5): R1431-R1438.

Morino K, Petersen KF, Dufour S, Befroy D, Frattini J, Shatzkes N, Neschen S, White MF, Bilz S, Sono S, Pypaert M, & Shulman GI. (2005). Reduced mitochondrial density and increased IRS-1 serine phosphorylation in muscle of insulin-resistant offspring of type 2 diabetic parents. J Clin Invest, 115: 3587–3593.

Morino K, Petersen KF, & Shulman GI. (2006). Molecular mechanisms of insulin resistance in humans and their potential links with mitochondrial dysfunction. Diabetes, 55(S2): S9-S15.

Morino K, Neschen S, Bilz S, Sono S, Tsirigotis D, Reznick RM, Moore I, Nagai Y, Samuel V, Sebastien D, White M, Philbrick W, & Shulman GI. (2008). Muscle-specific IRS-1 Ser→Ala transgenic mice are protected from fat-induced insulin resistance in skeletal muscle. Diabetes, 57: 2644-2651.

Mueckler M. (1994). Facilitative glucose transporters. Euro J Biochem, 219(3): 713-725.

Must A, Spadano J, Coakley EH, Field AE, Colditz G, Dietz WH. (1999). The disease burden associated with overweight and obesity. JAMA, 282: 1523–1529.

Mullen KL, Pritchard J, Ritchie I, Snook LA, Chabowski A, Bonen A, Wright D, & Dyck DJ. (2009). Adiponectin resistance precedes the accumulation of skeletal muscle lipids and insulin resistance in high-fat fed rats. Am J Physiol Integr Comp Physiol, 296: R243-R251.

Nesher M, & Boneh A. (1994). Effect of fatty acids and their acyl-CoA esters on protein kinase C activity in fibroblasts: possible implications in fatty acid oxidation defects. Biochim Biophys Acta, 1221: 66–72.

Norris S.M., R.A. Sayer, E. Bombardier, G.J. Babu, M. Periasamy, D.H. MacLennan, A.O. Gramolini, and A.R. Tupling (2008). Improved metabolic efficiency during sub-maximal exercise in mice lacking Sarcolipin (SLN). *Appl. Physiolo. Nutr. Metab.* 33(Supplement S1): S73

Norris SM, Bombardier E, Smith IC, Vigna C, & Tupling AR. (2009). ATP consumption by SR Ca^{2+} pumps accounts for 50% of resting metabolic rate in mouse fast and slow twitch skeletal muscle. Am J Physiol Cell Physiol, in press.

Oakes ND, Cooney GJ, Camilleri S, Chisholm DJ, Kraegen EW. (1997). Mechanisms of liver and muscle insulin resistance induced by chronic high-fat feeding. Diabetes, 46: 1768–1774.

Odermatt A, Becker S, Khanna VK, Kurzydlowski K, Leisner E, Pette D, & MacLennan DH. (1998). Sarcolipin regulates the activity of SERCA1, the fast-twitch skeletal muscle sarcoplasmic reticulum Ca2+-ATPase. J Biol Chem, 273(20): 12360-69.

Orellana A, Hidalgo PC, Morales MN, Mezzano D, & Bronfman M. (1990). Palmitoyl-CoA and the acyl-CoA thioester of the carcinogenic peroxisome- proliferator ciprofibrate potentiate diacylglycerol-activated protein kinase C by decreasing the phosphatidylserine requirement of the enzyme. Eur J Biochem, 190: 57–61.

Ouwens DM, Diamant M, Foddor M, Habets D, Pelsers MMAL, El Hanaoui M, Dang ZC, van den Brom CE, Vlasblom R, Rietdijk A, Boer C, Coort SML, Glatz JFC, & Luiken JJFP. (2007). Cardiac contractile dysfunction in insulin-resistant rats fed a high fat diet is associated with elevated CD36-mediated fatty acid uptake and esterification. Diabetologia, 50: 1938–1948.

Park CR, & Johnson LH (1955). Effect of insulin on transport of glucose and galactose into cells of rat muscle and brain. Am J Physiol, 182: 17–23.

Park SY, Cho YR, Kim HJ, Higashimori T, Danton C, Lee MK, Dey A, Rothermel B, Kim YB, Kalinowski A, Russell KS, & Kim JK. (2005). Unraveling the temporal pattern of diet-induced insulin resistance in individual organs and cardiac dysfunction i nC57BL/6 mice. Diabetes, 54: 3530-3540.

Paz K, Hemi R, LeRoith D, Karasik A, Elhanany E, Kanety H, & Zick Y. (1997). A molecular basis for insulin resistance. Elevated serine/threonine phosphorylation of IRS-1 and IRS-2 inhibits their binding to the juxtamembrane region of the insulin receptor and impairs their ability to undergo insulin-induced tyrosine phosphorylation. J Biol Chem, 272: 29911–29918.

Petersen KF, Dufour S, Befroy D, Garcia R, & Shulman GI. (2004). Impaired mitochondrial activity in the insulin-resistant offspring of patients with type 2 diabetes. N Engl J Med, 350: 664–671.

Perseghin G, Ghosh S, Gerow K, & Shulman GI. (1997). Metabolic defects in lean nondiabetic offspring of NIDDM parents: a cross-sectional study. Diabetes 46: 1001–1009.

Phillips SM, Green HJ, Tarnopolsky MA, Heigenhauser GJ, & Grant SM. (1996). Progressive effect of endurance training on metabolic adaptations in working skeletal muscle. Am J Physiol, 270: E265–E272.

Pickersgill L, Litherland GJ, Greenberg AS, Walker M, & Yeaman SJ. (2007). Key role for ceramides in mediating insulin resistance in human muscle cells. J Biol Chem, 282: 12583-12589.

Ploug T, Wojtaszewski J, Kristiansen S, Hespel P, Galbo H, & Richter E. (1993). Glucose transport and transporters in muscle giant vesicles: differential effects of insulin and contractions. Am J Physiol Endocrinol Metab, 264: E270–E278.

Prada PO, Zecchin HG, Gasparetti AL, Torsoni MA, Ueno M, Hirata AE, Corezola do Amaral ME, Höer NF, Boschero AC, Saad MJ. (2005). Western diet modulates insulin signaling, c-Jun N-terminal kinase activity, and insulin receptor substrate-1ser307 phosphorylation in a tissue-specific fashion. Endocrinol, 146(3): 1576-1587.

Prada PO, Ropelle ER, Mourao RH, de Souza CT, Pauli JR, Cintra DE, Schenka A, Rocco SA, Rittner R, Franchini KG, Vassallo J, Velloso LA, Carvalheira JB, & Saad MJ. (2009). EGFR tyrosine kinase inhibitor (PD153035) improves glucose tolerance and insulin action in high-fat diet-fed mice. Diabetes, 58: 2910-2919.

Rasmussen H. (1986). The calcium messenger system. N Engl J Med, 314: 1094-1101.

Ravichandran LV, Esposito DL, Chen J, Quon MJ. (2000). Protein kinase C phosphorylates insulin receptor subratrate-1 and impairs its ability to activate phosphatidylinositol 3-kinase in response to insulin, J Biol Chem, 276: 3543-3549.

Reaven GM, Hollenbeck C, Jeng CY, Wu MS, & Chen YD. (1988). Measurement of plasma glucose, free fatty acid, lactate, and insulin for 24h in patients with NIDDM. Diabetes, 37: 1020-1024.

Reaven GM. (1995). Pathophysiology of insulin resistance in human disease. Physiol Rev, 75(3): 473-483.

Ritov VB, Menshikova EV, He J, Ferrell RE, Goodpaster BH, & Kelley DE. (2005). Deficiency of subsarcolemmal mitochondria in obesity and type 2 diabetes. Diabetes, 54: 8-14.

Roe MW, Philipson LH, Frangakis CJ, Kuznetsov A, Mertz RJ, Lancaster ME, Spencer B, Worley JF, & Dukes ID. (1994). Defective glucose-dependent endoplasmic reticulum Ca2+ sequestration in diabetic mouse islets of Langerhans. J Biol Chem, 269: 18279–18282.

Rolfe DF, & Brown GC. (1997). Cellular energy utilization and molecular origin of standard metabolic rate in mammals. Physiol Rev, 77(3): 731-58.

Rowland ML. (1990). Self-reported weight and height. Am J Clin Nutr, 52(6): 1125-1133.

Saad MJ, Araki E, Miralpeix M, Rothenberg PL, White MF, & Kahn CR. (1992). Regulation of insulin receptor substrate-1 in liver and muscle of animal models of insulin resistance. J Clin Invest, 90(5): 1839-1849.

Sabin MA, Stewart CE, Crowne EC, Turner SJ, Hunt LP, Welsh GI, Grohmann MJ, Holly JM, & Shield JP. (2007). Fatty acid-induced defects in insulin signalling, in myotubes derived from children, are related to ceramide production from palmitate rather than the accumulation of intramyocellular lipid. J Cell Physiol, 211: 244-252.

Samuel VT, Liu ZX, Qu X, Elder BD, Bilz S, Befroy D, Romanelli AJ, & Shulman GI. (2004). Mechanism of hepatic insulin resistance in non-alcoholic fatty liver disease. J Biol Chem, 279(31): 32345-32353.

Sano H, Kane S, Sano E, Miinea CP, Asara JM, Lane WS, Garner CW, & Lienhard GE. (2003). Insulin-stimulated phosphorylation of a Rab GTPase-activating protein regulates GLUT4 translocation. J Biol Chem, 278(17): 14599-14602.

Santomauro A, Boden G, Silva M, Rocha DM, Santos RF, Ursich MJ, Strassmann PG, & Wajchenberg BL. (1999). Overnight lowering of free fatty acids with acipimox improves insulin resistance and glucose tolerance in obese diabetic and non-diabetic subjects. Diabetes, 48: 1836-1841.

Sarbassov DD, Guertin DA, Ali SM, & Sabatini DM. (2005). Phosphorylation and regulation of Akt/PKB by the Rictor- mTOR complex. Science, 307: 1098–1101.

Sayer RA, Bombardier E, Norris SM, Babu GJ, Periasamy M, MacLennan DH, Gramolini AO, & Tupling AR. (2008). Increased susceptibility to diet-induced obesity and glucose intolerance in mice lacking sarcolipin. Appl Physiol Nutr Metab, 33(S1): S89.

Schacterle GR, & Pollock RL. (1973). A simplified method for the quantitative assay of small amounts of protein in biological material. Analytical Biochem, 51: 654-655.

Schenk S, & Horowitz JF. (2007). Acute exercise increases triglyceride synthesis in skeletal muscle and prevents fatty acid-induced insulin resistance. J Clin Invest, 117: 1690-1698.

Schmitz-Peiffer C. (2000). Signalling aspects of insulin resistance in skeletal muscle: mechanisms induced by lipid oversupply. Cell Signal, 12: 583–594.

Schmitz-Peiffer C, Craig DL, Biden TJ. (1999). Ceramide generation is sufficient to account for the inhibition of the insulin-stimulated PKB pathway in C2C12 skeletal muscle cells pretreated with palmitate. J Biol Chem, 274: 24202–24210.

Schrauwen P. (2007). High-fat diet, muscular lipotoxicity and insulin resistance. Proc Nutr Soc, 66: 33-41.

Seidler NW, Jona I, Vegh M & Martonosi A. (1989). Cyclopiazonic acid is a specific inhibitor of the Ca^{2+}-ATPase of sarcoplasmic reticulum. J Biol Chem, 264: 17816-17823.

Shima K, Shi K, Sano T, Iwami T, Mizuno A, & Noma Y. (1993). Is exercise training effective in preventing diabetes mellitus in the Otsuka-Long-Evans-Tokushima fatty rat, a model of spontaneous non-insulin dependent diabetes mellitus. Metabolism, 42(8): 971-977.

Shoelson SE, Chatterjee S, Chaudhuri M, & White MF. (1992). YMXM motifs of irs-1 define substrate specificity of the insulin receptor kinase. Proc Natl Acad Scit USA, 89(6): 2027-2031.

Shulman GI. (2000). Molecular mechanisms of insulin resistance. J Clin Invest, 106(2): 171-176.

Shulman GI, Rothman DL, Jue T, Stein P, DeFronzo RA, & Shulman RG. (1990). Quantitation of muscle glycogen synthesis in normal subjects and subjects with non-insulin dependent diabetes by 13C nuclear magnetic resonance spectroscopy. N Engl J Med, 322(4): 223-228.

Sims EAH, Danforth Jr. E, Horton ES, Bray GA, Glennon JA, & Salans LB. (1973). Endocrine and metabolic effects of experimental obesity in man. Recent Prog Horm Res, 29: 457-496.

Smith WS, Broadbridge R, East JM, & Lee AG. (2002). Sarcolipin uncouples hydrolysis of ATP from accumulation of Ca2+ by the Ca2+-atpase of skeletal-muscle sarcoplasmic reticulum. J Biochem, 361: 277-86.

Smith AC, Mullen KL, Junkin KA, Nickerson J, Chabowski A, Bonen A, & Dyck DJ. (2007). Metformin and exercise reduce muscle FAT/CD36 and lipid accumulation and blunt theprogression of high-fat diet induced hyperglycemia. Am J Physiol Endocrinol Metab 293: E172–E181.

Sparks LM, Xie H, Koza RA, Mynatt R, Hulver MW, Bray GA, & Smith SR. (2005). A high fat diet co-ordinately downregulates genes required for mitochondrial oxidative phosphorylation in skeletal muscle. Diabetes, 54: 1926-1933.

Straczkowski M, Kowalska I, Baranowski M, Nikolajuk A, Otziomek E, Zabielski P, Adamska A, Blachnio A, Gorski J, & Gorska M. (2007). Increased skeletal muscle ceramide level in men at risk of developing type 2 diabetes. Diabetologia, 50: 2366-2373.

Stratford S, Hoehn KL, Liu F, & Summers SA. (2004). Regulation of insulin action by ceramide: dual mechanisms linking ceramide accumulation to the inhibition of Akt/protein kinase B. J Biol Chem, 279: 36608–36615.

Sun XJ, Rothenberg P, Kahn CR, Backer JM, Araki W, Wilden PA, Cahill DA, Goldstein BJ, & White MF. (1991). Structure of the insulin receptor substrate IRS-1 defines a unique signal transduction protein. Nature, 352(6330): 73-77.

Suzuki K, & Kono T. (1980). Evidence that insulin causes translocation of glucose transport activity to the plasma membrane from an intracellular storage site. PNAS, 77: 2542–2545.

Tanti JF, Grillo S, Gremeaux T, Coffer PJ, Van Obberghen E, & Le Marchand-Brustel Y. (1997). Potential role of protein kinase B in glucose transporter 4 translocation in adipocytes. Endcrin, 138: 2005-2010.

Taylor BA, & Phillips SJ. (1996). Detection of obesity QTLs on mouse chromosomes 1 and 7 by selective DNA pooling. Genomics, 34: 389-398.

Thompson AL, Lim-Fraser MY, Kraegen EW, & Cooney GJ. (2000). Effects of individual fatty acids on glucose uptake and glycogen synthesis in soleus muscle in vitro. Am J Physiol Endocrinol Metab, 279: E577–E584.

Timmers S, SchrauwenP, & de Vogel J. (2007). Muscular diacylglycerol metabolism and insulin resistance. Physiol Behav, 94: 242-251.

Tjepkema M. (2006). Adult obesity. Health Reports, 17(3): 9-25.

Toyoshima C. (2008). Structural aspects of ion pumping by Ca^{2+}-ATPase of sarcoplasmic reticulum. Arch Biochem Biophys, 476: 3-11.

Tupling, A.R. (2004). The sarcoplasmic reticulum in muscle fatigue and disease: Role of the sarco(endo)plasmic reticulum Ca2+-ATPase. Can J Appl Physiol, 29(3): 308-329.

Turcotte LP, Swenberger JR, Tucker MZ, & Yee AJ. (2001). Increased fatty acid uptake and altered fatty acid metabolism in insulin resistant muscle of obese Zucker rats. Diabetes 50: 1389–1396.

Turinsky J, O'Sullivan DM, & Bayly BP. (1990). 1,2-Diacylglycerol and ceramide levels in insulin-resistant tissues of the rat in vivo. J Biol Chem, 265: 16880–16885.

Turner N, Bruce CR, Beale SM, Hoehn KL, So T, Rolph MS, & Cooney GJ. (2007). Excess lipid availability increases mitochondrial fatty acid oxidative capacity in muscle: evidence against a role of reduce fatty acid oxidation in lipid-induced insulin resistance in rodents. Diabetes, 56: 2085-2092.

Ueki K, Fruman DA, Brachmann SM, Tseng YH, Cantley LC, & Kahn CR. (2002). Molecular balance between the regulatory and catalytic subunits of phosphoinositide 3-kinase regulates cell signalling and survival. Mol Cell Biol, 22: 965–977.

Ueki K, Fruman DA, Yballe CM, Fasshauer M, Klein J, Asano T, Cantley LC, & Kahn CR. (2003). Positive and negative roles of p85a and p85b regulatory subunits of phosphoinositide 3-kinase in insulin signalling. J Bio Chem, 278(48): 48453-48466.

Wang H, Knaub LA, Jensen DR, Young Jung D, Hong EG, Ko HJ, Coates AM, Goldberg IJ, de la Houssaye BA, Janssen RC, McCurdy CE, Rahman SM, Soo Choi C, Shulman GI, Kim JK, Friedman JE, & Eckel RH. (2009). Skeletal muscle-specific deletion of lipoprotein lipase enhances insulin signaling in skeletal muscle but causes insulin resistance in liver and other tissues. Diabetes, 58: 116-124.

Warram JH, Martin BC, Krolewski AS, Soeldner JS, & Kahn CR. (1990). Slow glucose removal rate and hyperinsulinemia precede the development of type II diabetes in the offspring of diabetic parents. Ann Intern Med, 113(12): 909-915.

Wawrzynow A, Theibert JL, Murphy C, Jona I, Martonosi A, & Collins JH. (1992). Sarcolipin, the proteolipid of skeletal muscle sarcoplasmic reticulum, is a unique, amphipathic, 31-residue peptide. Arch Biochem Biophys, 298(2): 620-623.

Wild S, Roglic G, Green A, Sicree R, & King H. (2004). Global prevalence of diabetes – estimates for the year 2000 and projections for 2030. Diabetes Care, 27(5): 1047-53.

Wilkes J, Bonen A, & Bell RC. (1998). A modified high-fat diet induces insulin resistance in rat skeletal muscle but not adipocytes. Am J Physiol Endocrinol Metab, 275: E679-E686.

Withers DJ, Guiterrez JS, Towery H, Burks DJ, Ren JM, Previs S, Zhang Y, Bernal D, Pons S, Shulman GI, Bonner-Weir S, & White MF. (1998). Disruption of irs-2 causes type 2 diabetes in mice. Nature, 391: 900-904.

Young ME, Guthrie PH, Razeghi P, Leighton B, Abbasi S, Patil S, Youker KA, & Taegtmeyer H. (2002). Impaired long-chain fatty acid oxidation and contractile dysfunction in the obese Zucker rat heart. Diabetes 51: 2587–2595.

Yu CL, Chen Y, Cline GW, Zhang DY, Zong HH, Wang YL, Bergeron R, Kim JK, Cushman SW, Cooney GJ, Atcheson B, White MF, Kraegen EW, Shulman GI. (2002). Mechanism by which fatty acids inhibit insulin activation of insulin receptor substrate-1 (IRS-1)-associated phosphatidylinositol 3-kinase activity in muscle. J Biol Chem 277:50230 –50236.

Zerial M, & McBride H. (2001). Rab proteins as membrane organizers. Nat Rev Mol Cell Biol, 2: 107–119.

Zhang SJ, Anderson DC, Sandstrom SM, Westerblad H and Katz A. (2006). Cross bridges account for only 20% of total ATP consumption during submaximal isometric contraction in mouse fast-twitch skeletal muscle. Am J Physiol, 291: C147-C154.

Zhoa J, Zhang N, He M, Yang Z, Tong W, Wang Q, & Hu R. (2008). Increased beta-cell apoptosis and impaired insulin signalling pathway contributes to the onset of diabetes in OLETF rats. Cell Physiol Biochem, 21(5-6): 445-454.

Zurlo F, Larson K, Bogarduc C, & Ravussin E. (1990). Skeletal muscle metabolism is a major determinant of resting energy expenditure. J Clin Invest, 86(5): 1423-1427

Appendix A: Product Sheet of Chow Diet

8640
Harlan Teklad 22/5 Rodent Diet

Product Description—Harlan Teklad 22/5 Rodent Diet is an economical, complete, and balanced fixed formula diet designed to provide consistent nutrition to research rodents. Also recommended for use with hamsters.

Ingredients—Dehulled soybean meal, ground corn, wheat middlings, flaked corn, fish meal, cane molasses, soybean oil, ground wheat, dried whey, dicalcium phosphate, brewers dried yeast, calcium carbonate, iodized salt, choline chloride, magnesium oxide, vitamin A acetate, vitamin D_3 supplement, vitamin E supplement, niacin, calcium pantothenate, riboflavin, thiamine mononitrate, pyridoxine hydrochloride, menadione sodium bisulfite complex (source of vitamin K activity), folic acid, biotin, vitamin B_{12} supplement, manganous oxide, ferrous sulfate, copper sulfate, zinc oxide, calcium iodate, cobalt carbonate, chromium potassium sulfate, kaolin.

Guaranteed Analysis		
Crude Protein	(Min.)	22.0%
Crude Fat	(Min.)	5.0%
Crude Fiber	(Max.)	4.5%
Average Nutrient Composition		
Protein	%	22.58
Fat	%	5.23
Fiber	%	3.94
Ash	%	7.06
Nitrogen-Free Extract	%	51.19
Gross Energy	Kcal/g	3.62
Digestible Energy	Kcal/g	3.38
Metabolizable Energy	Kcal/g	3.11
Linoleic Acid	%	3.32
Amino Acids		
Arginine	%	1.65
Methionine	%	0.37
Cystine	%	0.37
Histidine	%	0.52
Isoleucine	%	1.17
Leucine	%	1.88
Lysine	%	1.29
Phenylalanine + Tyrosine	%	2.04
Threonine	%	0.93
Tryptophan	%	0.29
Valine	%	1.17

Minerals		
Calcium	%	1.13
Phosphorus	%	0.94
Sodium	%	0.40
Chlorine	%	0.67
Potassium	%	1.00
Magnesium	%	0.24
Iron	mg/Kg	348.75
Manganese	mg/Kg	104.19
Zinc	mg/Kg	78.84
Copper	mg/Kg	24.07
Iodine	mg/Kg	2.69
Cobalt	mg/Kg	0.72
Selenium	mg/Kg	0.26
Vitamins		
Vitamin A	IU/g	15.99
Vitamin D_3	IU/g	2.99
Vitamin E	IU/Kg	109.54
Choline	mg/g	2.39
Niacin (Nicotinic Acid)	mg/Kg	65.61
Pantothenic Acid	mg/Kg	22.51
Pyridoxine (Vitamin B_6)	mg/Kg	14.45
Riboflavin (Vitamin B_2)	mg/Kg	6.56
Thiamine (Vitamin B_1)	mg/Kg	32.62
Menadione (Vitamin K_3)	mg/Kg	5.22
Folic Acid	mg/Kg	3.19
Biotin	mg/Kg	0.42
Vitamin B_{12}(Cyanocobalamin)	mcg/Kg	54.60
Vitamin C	mg/Kg	---

Reported nutrient values may vary due to the inherent variability in laboratory analysis.

www.teklad.com • customerservice@teklad.com • 1-800-483-5523

2/16/2006

Appendix B: Product Sheet of High-Fat Diet

Harlan Teklad — *Custom Research Diets*

TD.88137 Adjusted Calories Diet (42% from fat)

Formula	g/Kg
Casein	195.0
DL-Methionine	3.0
Sucrose	341.46
Corn Starch	150.0
Anhydrous Milkfat	210.0
Cholesterol	1.5
Cellulose	50.0
Mineral Mix, AIN-76 (170915)	35.0
Calcium Carbonate	4.0
Vitamin Mix, Teklad (40060)	10.0
Ethoxyquin, antioxidant	0.04

Key Planning Information

- *Products are made fresh to order*
- Store product at 4°C or lower
- Recommended use within 3 months
- Box labeled with product name, manufacturing date, and lot number
- Lead time:
  - Up to 2 weeks non-irradiated
  - Up to 4 weeks irradiated

Footnote

TD 88137 is often referred to as the Western Diet in the cardiovascular literature. The overall level of fat and the saturated nature of the fat are representative of diets that are linked to risk of cardiovascular disease in humans. The formula originated with researchers at Rockefeller University and is used primarily with genetically manipulated mouse models that are susceptible to atherosclerosis. The diet may also be useful in diet induced obesity, diabetes, and metabolic syndrome models.

Product Specific Information

- 1/2" Pellet or Powder (crumbly)
- Minimum order 3 Kg
- Irradiation available upon request
- Feed fresh diet at minimum one time per week (discard unused diet)

Related Diets

There are numerous modifications of TD 88137. Contact a nutritionist for more information about specific modifications, or to develop one that suits your needs.

Options (Fees Will Apply)

- Rush order (pending availability)
- Irradiation (see Product Specific Information)
- Vacuum packaging (0.5, 1, 2 Kg)

Selected Nutrient Information [1]

	% by weight	% kcal from
Protein	17.3	15.2
Carbohydrate	48.5	42.7
Fat	21.2	42.0

Kcal/g	**4.5**
Cholesterol [2]	**0.2%**

[1] Values are calculated from ingredient analysis or manufacturer data

[2] 0.15% added, 0.05% from fat source

International Inquiry

·*Outside U.S.A. or Canada*·

- **askanutritionist@teklad.com**

Speak With A Nutritionist

- **800·483·5523**
- **askanutritionist@teklad.com**

Place Your Order (U.S.A. & Canada)

· *Place Order* · *Obtain Pricing* · *Check Order Status* ·

- **800·483·5523**
- **608·277·2066** *facsimile*
- **customerservice@teklad.com**

Harlan TEKLAD — P.O. Box 44220 · Madison, WI 53744-4220 · 800 · 483 · 5523 — *Access to excellence*

Appendix B: Product Sheet of High-Fat Diet

Harlan TEKLAD

TD.88137 - Adjusted Calories Diet (42% from fat)

Typical Fatty Acid Analysis

		Mean	SD
Saturated fat	% of diet	13.3	0.8
Monounsaturated fat	% of diet	5.9	0.6
Polyunsaturated fat	% of diet	0.9	0.4
Unknown	% of diet	0.9	0.2
Total	% of diet	20.8	0.1

Typical Profile

4:0	% of total fatty acids	1.2	0.1
6:0	% of total fatty acids	1.2	0.1
8:0	% of total fatty acids	0.9	0.1
10:0	% of total fatty acids	2.3	0.1
12:0	% of total fatty acids	3.0	0.3
14:0	% of total fatty acids	10.3	0.8
14:1	% of total fatty acids	0.8	0.1
15:0	% of total fatty acids	1.2	0.2
16:0	% of total fatty acids	29.4	1.3
16:1	% of total fatty acids	1.7	0.1
17:0	% of total fatty acids	0.8	0.1
18:0	% of total fatty acids	12.6	0.8
18:1 (Oleic)	% of total fatty acids	20.7	2.5
18:1 Isomers	% of total fatty acids	4.7	0.2
18:2 (Linoleic)	% of total fatty acids	2.3	1.0
18:2 Isomers	% of total fatty acids	1.0	0.2
18:3 (Linolenic)	% of total fatty acids	0.6	0.2
Others*	% of total fatty acids	5.1	1.1

Compilation of analytical data

n = 11

*Others are a combination of unidentified fatty acids and those contributing on average less than 0.5% of total fatty acids, such as EPA and DHA.

11/1/2007

PO BOX 44220 Madison, WI 53744-4220 Phone: (608) 277-2070 Fax: (608) 277-2066
www.tekladcustomdiets.com